

# **BLDC Motor-Driven Grid Interfaced Solar PV Based Water Pumping Using Zeta Converter**

*A dissertation*

*Submitted in partial fulfillment of the requirements*

*For the award of the degree of*

**Master of Technology**

**In**

**Power Electronics & Drives**

Submitted by

**K VIJAYA DATTU**

**(19NK1D5207)**

**Under the esteemed guidance of**

**Mr. A. ARUN KUMAR M.Tech**

**Associate professor**



**Department of Electrical and Electronics Engineering**

**VELAGA NAGESWARA RAO COLLEGE OF ENGINEERING**

**(Affiliated to JNT University, Kakinada)**

**PONNURU- 522 124**

**2019-2021**

**VELAGA NAGESWARA RAO COLLEGE OF ENGINEERING**  
**(AFFILIATED TO JNT UNIVERSITY, KAKINADA)**  
**PONNURU- 522 124**  
**ANDHRA PRADESH**



**CERTIFICATE**

This is to certify that the project work entitled “**BLDC Motor-Driven Grid Interfaced Solar PV Based Water Pumping Using Zeta Converter**” that is being submitted by **K VIJAYA DATTU (19NK1D5207)** in partial fulfillment of the requirement of **MASTER OF TECHNOLOGY IN POWER ELECTRONICS&DRIVES** to the **VELAGA NAGESWARA RAO COLLEGE OF ENGINEERING** during the year 2018-2020 is carried out by him under my guidance and supervision.

**Internal Guide**

**Sri. A. ARUN KUMAR M.Tech**

Associate professor & HOD  
Dept. of EEE

**Head of Department**

**Sri. A. ARUN KUMAR M.Tech**

Associate professor & HOD  
Dept. of EEE

**External Examiner**

## DECLARATION

The accompanying thesis entitled **“BLDC Motor-Driven Grid Interfaced Solar PV Based Water Pumping Using Zeta Converter”** is submitted for **Master of Technology (Power Electronics and Drives)** at the **Velaga Nageswara Rao college of engineering, Ponnur**. I declare this is my original work supervision of Mr. **Sri. A. ARUN KUMAR**. All the work ideas recorded are original where acknowledged in the text or reference. The work presented here has not previously been submitted for a degree or diploma at this or any other, University or Examining body.

**K VIJAYA DATTU**  
**(19NK1D5207)**

## ACKNOWLEDGEMENTS

I would like to express my deepest sense of gratitude towards my supervisor, **Sri. A. ARUN KUMAR M.Tech**, Associate Professor in Department of EEE, for his essential advices and helping out in grasping the crux of my project.

I privileged to express my sincere gratitude to the Head of the Department **Associate Prof.A.ARUN KUMAR** for giving his continuous support and guidance in my endeavor.

I would like to thank **Project Review Committee & all the staff members** of Department of EEE for their extended cooperation and guidance.

I take the opportunity to express my heartfelt gratitude to the Principal **Dr.Y.RAMESH BABU** who has given support for the project or in other aspects of my studies at VNR College of Engineering & Technology.

I will be failing in my duty if I do not mention the laboratory staff of this department for their timely help.

Finally, Special Thanks to all my friends, without their unwavering support, love, and understanding, I would have never been able to complete this journey.

**K VIJAYA DATTU**  
**(19NK1D5207)**

# INDEX

TOPICS	PAGE NO.S
LIST OF CONTENTS	i
LIST OF FIGURES	iv
<b>CHAPTER 1 INTRODUCTION</b>	<b>1</b>
1.1 BLDC Motor	1
1.2 Operation	2
1.3 Photovoltaic Technology	4
1.4 Classification of PV System	6
1.4.1 PV cell	7
1.4.2 PV Module	7
1.4.3 Array	8
1.5 Voltage Source Inverters	10
1.6 Single-Phase Voltage Source Inverters	12
1.7 Half-Bridge VSI	12
1.8 Full-Bridge VSI	13
1.9 Three Phase Voltage Source Inverters	14
1.10 Maximum Power Point Tracking	15
1.10.1 I-V curve	17
1.11 Classification	18
1.11.1 Perturb and observe	18
1.11.2 Incremental conductance	19
1.11.3 Current sweep	20
1.11.4 Constant voltage	20
1.11.5 Comparison of methods	21
1.11.6 MPPT placement	22
1.11.7 Operation with batteries	22
1.12 Water Pumps	22
1.12.1 Centrifugal Pumps	23
1.12.2 Volumetric Pumps	24

1.13	ZETA Converter	24
1.13.1	Modes of Operation	24
<b>CHAPTER 2</b>	<b>LITERATURE SURVEY</b>	<b>26</b>
2.1	DC-to-DC Converter with Low Input Current Ripple for Maximum Photovoltaic Power Extraction	26
2.1.1	Effect of Input Current Ripple	27
2.2	A Comparative Study on Maximum Power Point Tracking Techniques for Photovoltaic Power Systems	29
2.2.1	Review on MPPT Techniques	30
2.3	Evaluation of the Main MPPT Techniques for Photovoltaic Applications	31
<b>CHAPTER 3</b>	<b>PROPOSED CONCEPT</b>	<b>35</b>
3.1	Introduction	35
3.2	Configuration of Proposedsystem	37
3.3	Operation of Proposedsystem	38
3.4	Design of Proposedsystem	39
3.4.1	Design of SPV Array	39
3.4.2	Design of Zeta Converter	40
3.4.3	Estimation of DC-Link Capacitor of VSI	41
3.4.4	Design of Water Pump	42
3.5	Control of Proposed System	43
3.5.1	INC-MPPT Algorithm	43
3.5.2	Electronic Commutation of BLDC Motor	44
<b>CHAPTER 4</b>	<b>MATLAB AND SIMULATION MODEL</b>	<b>46</b>
4.1	Introduction to MATLAB	46
4.2	Proposed Work	48
4.2.1	Importance of Fuzzy Logic	48
4.2.2	Usage of Fuzzy Logic	48
4.2.3	Convenience of Fuzzy Logic	49
4.2.4	The Fuzzy Logic Concept	49
4.2.5	Fuzzification	52

4.2.6	Defuzzification	52
4.2.7	Fuzzy Logic Controller	52
4.3	MATLAB/SIMULINK Results:	53
<b>CHAPTER 5 CONCLUSION</b>		<b>58</b>
<b>REFERENCES</b>		<b>59</b>

## LIST OF FIGURES

S.NO	FIGURE NO.S	PAGE NO.S
1.1	BLDC motor transverse section	2
1.2	Ideal back-emf's, phase currents, and position sensor signals	3
1.3	BLDC motor cross section and phase energizing sequence	3
1.4	Simplified BLDC drive scheme	4
1.5	Photovoltaic system	6
1.6	Classification of PV systems	6
1.7	Structure of a PV cell	7
1.8	Structure of a PV module with 36 cells connected in series	8
1.9	Structure of a PV array	9
1.10	Model of PV cell	10
1.11	(a) The electrical power conversion topology	11
1.11	(b) The ideal input (ac mains) and output (load) waveforms	12
1.11	(c) The actual input (ac mains) and output (load) waveforms	12
1.12	Single-phase half-bridge VSI	13
1.13	Single-phase full-bridge VSI	14
1.14	Three-phase VSI topology	15
1.15	Photovoltaic solar cell I-V curves where a line intersects the knee of the curves where the maximum power transfer point is located	17
1.16	Perturb and observe algorithm	18
1.17	Flowchart Perturb and observe algorithm	19
1.18	Incremental conductance algorithm	20
1.19	Basic Zeta converter circuit	24
1.20	Equivalent circuit of converter (switch ON)	25
1.21	Equivalent circuit of converter (switch OFF)	25
2.1	Effect of the input current ripple on the dc power supply	28
2.2	Effect of input current ripple on the PV power curve	29
2.3	(a) I-V and (b) P-V characteristics of PV panel at different environmental Conditions	30



2.4	Block diagram of OCC technique	31
2.5	PV current-versus-voltage characteristic	33
3.1	Conventional SPV-fed BLDC motor-driven water pumping system	36
3.2	Proposed SPV-zeta converter-fed BLDC motor drive for water pump	38
3.3	Illustration of INC-MPPT with SPV array $P_{pv} - V_{pv}$ characteristics	42
4.1	Fuzzy inference system	51
4.2	Matlab/Simulink circuit of Starting and steady-state performances of the proposed SPV array based zeta converter-fed BLDC motor drive for water pump	52
4.3	Starting and steady-state performances of the proposed SPV arraybased zeta converter-fed BLDC motor drive for water pump. (a) SPV arrayvariables. (b) Zeta converter variables. (c) BLDC motor-pump variables	54
4.4	Matlab/Simulink circuit for Dynamic performance of SPV array-based zeta converter-fed BLDC motor drive for water pump	54
4.5	Dynamic performances of the proposed SPV array-based zeta converter-fed BLDC motor drive for water pump. (a) SPV array variables. (b) Zeta converter variables. (c) BLDC motor-pump variables.	56

**Abstract:** In this project zeta converter-fed brushless direct current (BLDC) motor drive as a cost-effective solution for low-power applications is presented. The VSI, converting dc output from a zeta converter into ac, feeds the BLDC motor to drive a water pump coupled to its shaft. The VSI is operated in fundamental frequency switching through an electronic commutation of BLDC motor assisted by its built-in encoder. The high frequency switching losses are thereby eliminated, contributing in an increased efficiency of proposed water pumping system. By adjusting the dc link voltage of the voltage source inverter (VSI) feeding a BLDC motor, the speed of the BLDC motor is controlled. This paper deals with the implementation of pulse width modulated Zeta converter, lower total harmonic distortion factor and better efficiency. The proposed zeta converter based BLDC Motor drive is implemented to improve the efficiency of water pumping system and to obtain a wide range of speed control.

Index Terms—Brushless dc (BLDC) motor, incremental conductance maximum power point tracking (INC-MPPT), solar photovoltaic (SPV) array, voltage-source inverter (VSI), water pump, zeta converter

# **CHAPTER 1**

## **INTRODUCTION**

### **1.1 BLDC MOTOR**

A BLDC motor is a permanent magnet synchronous that uses position detectors and an inverter to control the armature currents. The BLDC motor is sometimes referred to as an inside out dc motor because its armature is in the stator and the magnets are on the rotor and its operating characteristics resemble those of a dc motor. Instead of using a mechanical commutator as in the conventional dc motor, the BLDC motor employs electronic commutation which makes it a virtually maintenance free motor.

There are two main types of BLDC motors: trapezoidal type and sinusoidal type. In the trapezoidal motor the back-Emf induced in the stator windings has a trapezoidal shape and its phases must be supplied with quasi-square currents for ripple free operation. The sinusoidal motor on the other hand has a sinusoidally shaped back – emf and requires sinusoidal phase currents for ripple free torque operation. The shape of the back – emf is determined by the shape of rotor magnets and the stator winding distribution.

The sinusoidal motor needs high resolution position sensors because the rotor position must be known at every time instant for optimal operation. It also requires more complex software and hardware. The trapezoidal motor is a more attractive alternative for most applications due to simplicity, lower price and higher efficiency.

BLDC motors exist in many different configurations but the three phase motor is most common type due to efficiency and low torque ripple. This type of motor also offers a good compromise between precise control and number of power electronic devices needed to control stator currents. Fig. 2.1 shows a transverse section of a BLDC motor. Position detection is usually implemented using three Hall - an effect sensor that detects the presence of small magnets that are attached to the motor shaft.

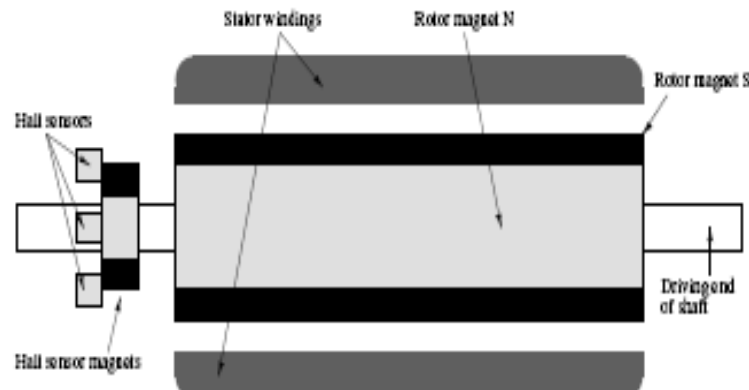


Fig.1.1 BLDC motor transverse section.

## 1.2 OPERATION

Typically, a Brushless dc motor is driven by a three-phase inverter with, what is called, six-step commutation. The conducting interval for each phase is  $120^\circ$  by electrical angle. The commutation phase sequence is like AB-AC-BC-BA-CA-CB. Each conducting stage is called one step. Therefore, only two phases conduct current at any time, leaving the third phase floating. In order to produce maximum torque, the inverter should be commutated every  $60^\circ$  so that current is in phase with the back EMF. The commutation timing is determined by the rotor position, which can be detected by Hall sensors as shown in the figure 1.2 (H1, H2, H3). The figure also shows ideal currents and back emf waveforms.

Figure 1.2 shows a cross section of a three phase star connected motor along with its phase energizing sequence. Each interval starts with the rotor and stator field lines  $120^\circ$  apart and ends when they are  $60^\circ$  apart. Maximum torque is reached when the field lines are perpendicular. Current commutation is done by inverter as shown in a simplified form in figure. The switches are shown as bipolar junction transistors but MOSFET switches are more common. Table 1.1 shows the switching sequence, the current direction and the position sensor signals.

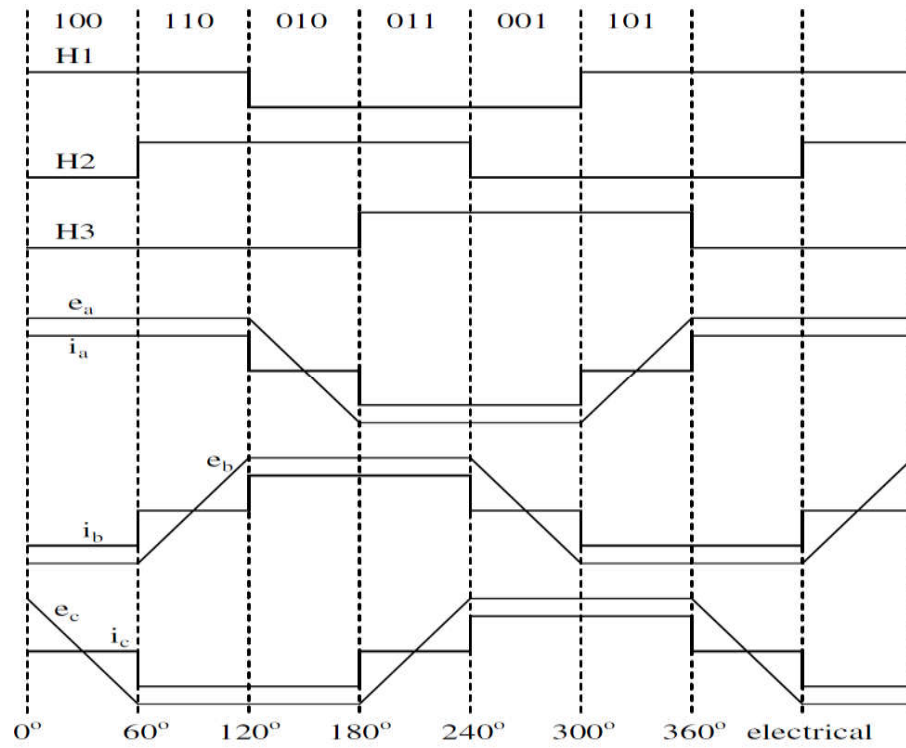


Fig.1.2 Ideal back-emf's, phase currents, and position sensor signals.

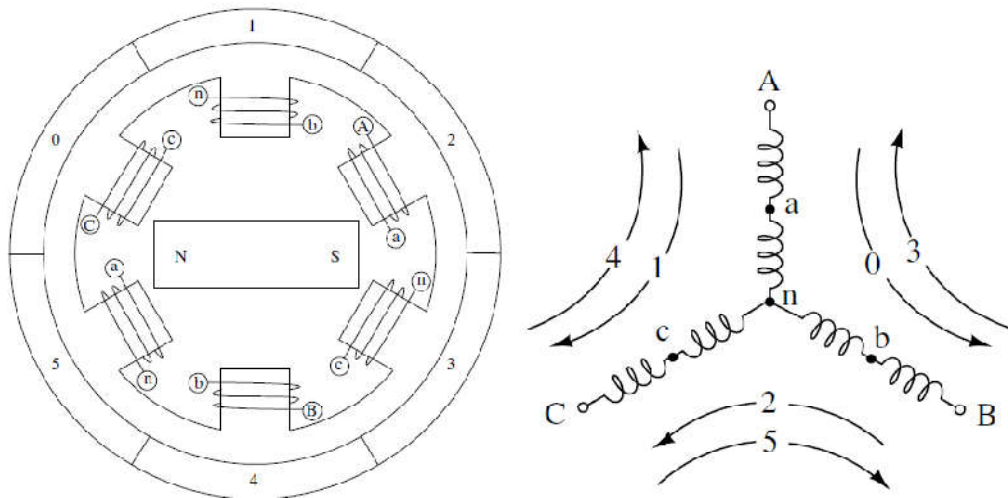


Fig.1.3: BLDC motor cross section and phase energizing sequence

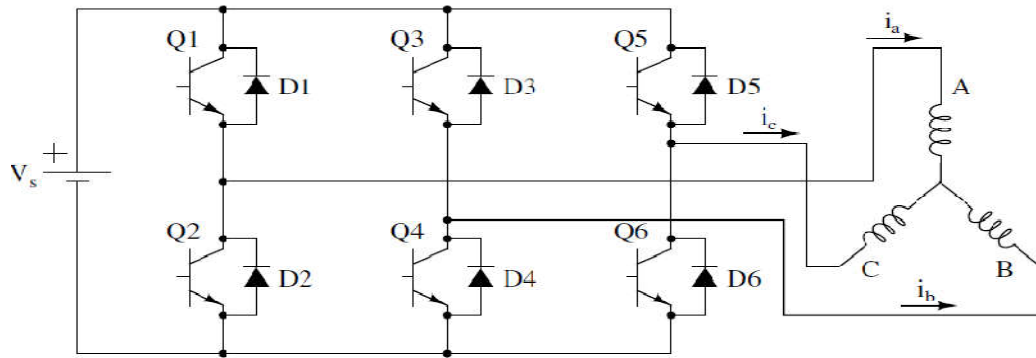


Fig.1.4: Simplified BLDC drive scheme

Table1.1: Switching Sequence.

Switching interval	Seq. number	Pos. sensors			Switch closed		Phase Current		
		H1	H2	H3			A	B	C
$0^\circ - 60^\circ$	0	1	0	0	Q1	Q4	+	-	off
$60^\circ - 120^\circ$	1	1	1	0	Q1	Q6	+	off	-
$120^\circ - 180^\circ$	2	0	1	0	Q3	Q6	off	+	-
$180^\circ - 240^\circ$	3	0	1	1	Q3	Q2	-	+	off
$240^\circ - 300^\circ$	4	0	0	1	Q5	Q2	-	off	+
$300^\circ - 360^\circ$	5	1	0	1	Q5	Q4	off	-	+

### 1.3PHOTOVOLTAIC TECHNOLOGY

A PV array consists of a number of PV modules, mounted in the same plane and electrically connected to give the required electrical output for the application. The PV array can be of any size from a few hundred watts to hundreds of kilowatts, although the larger systems are often divided into several electrically independent sub arrays each feeding into their own power conditioning system.

Photovoltaic's is the field of technology and research related to the devices which directly convert sunlight into electricity using semiconductors that exhibit the photovoltaic effect. Photovoltaic effect involves the creation of voltage in a material upon exposure to electromagnetic radiation.

The photovoltaic effect was first noted by a French physicist, Edmund Becquerel, in 1839, who found that certain materials would produce small amounts of electric current when exposed to light. In 1905, Albert Einstein described the nature of light and the photoelectric effect on which photovoltaic technology is based, for which he later

won a Nobel prize in physics. The first photovoltaic module was built by Bell Laboratories in 1954. It was billed as a solar battery and was mostly just a curiosity as it was too expensive to gain widespread use. In the 1960s, the space industry began to make the first serious use of the technology to provide power aboard spacecraft. Through the space programs, the technology advanced, its reliability was established, and the cost began to decline. During the energy crisis in the 1970s, photovoltaic technology gained recognition as a source of power for non-space applications.

The solar cell is the elementary building block of the photovoltaic technology. Solar cells are made of semiconductor materials, such as silicon. One of the properties of semiconductors that makes them most useful is that their conductivity may easily be modified by introducing impurities into their crystal lattice. For instance, in the fabrication of a photovoltaic solar cell, silicon, which has four valence electrons, is treated to increase its conductivity. On one side of the cell, the impurities, which are phosphorus atoms with five valence electrons (n-donor), donate weakly bound valence electrons to the silicon material, creating excess negative charge carriers.

On the other side, atoms of boron with three valence electrons (p-donor) create a greater affinity than silicon to attract electrons. Because the p-type silicon is in intimate contact with the n-type silicon a p-n junction is established and a diffusion of electrons occurs from the region of high electron concentration (the n-type side) into the region of low electron concentration (p-type side). When the electrons diffuse across the p-n junction, they recombine with holes on the p-type side.

However, the diffusion of carriers does not occur indefinitely, because the imbalance of charge immediately on either sides of the junction originates an electric field. This electric field forms a diode that promotes current to flow in only one direction.

Ohmic metal-semiconductor contacts are made to both the n-type and p-type sides of the solar cell, and the electrodes are ready to be connected to an external load. When photons of light fall on the cell, they transfer their energy to the charge carriers. The electric field across the junction separates photo-generated positive charge carriers (holes) from their negative counterpart (electrons). In this way an electrical current is extracted once the circuit is closed on an external load.

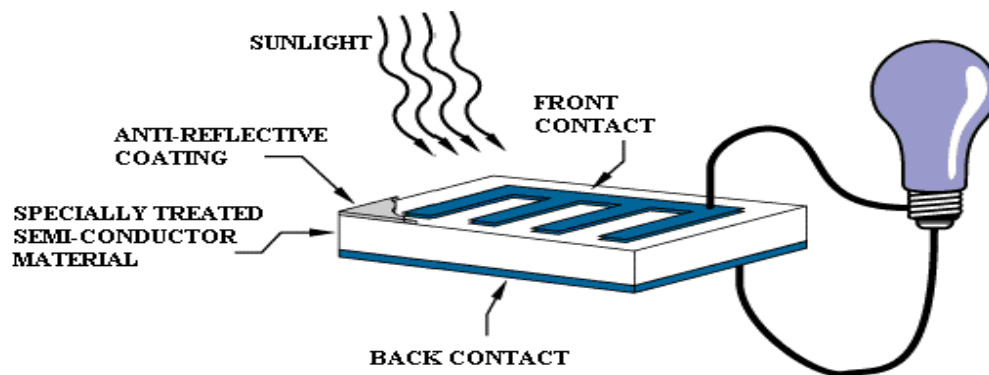


Fig:1.5 Photovoltaic system

#### 1.4 CLASSIFICATION OF PV SYSTEM

Figure 1.6. The two main general classifications as depicted in the figure are the stand-alone and the grid-connected systems. The main distinguishing factor between these two systems is that in stand-alone systems the solar energy output is matched with the load demand. To cater for different load patterns, storage elements are generally used and most systems currently use batteries for storage. If the PV system is used in conjunction with another power source like a wind or diesel generator then it falls under the class of hybrid systems. The balance of system (BOS) components are a major contribution to the life cycle costs of a photovoltaic system. They include all the power conditioning units, storage elements and mechanical structures that are needed. They especially have a huge impact on the operating costs of the PV system.

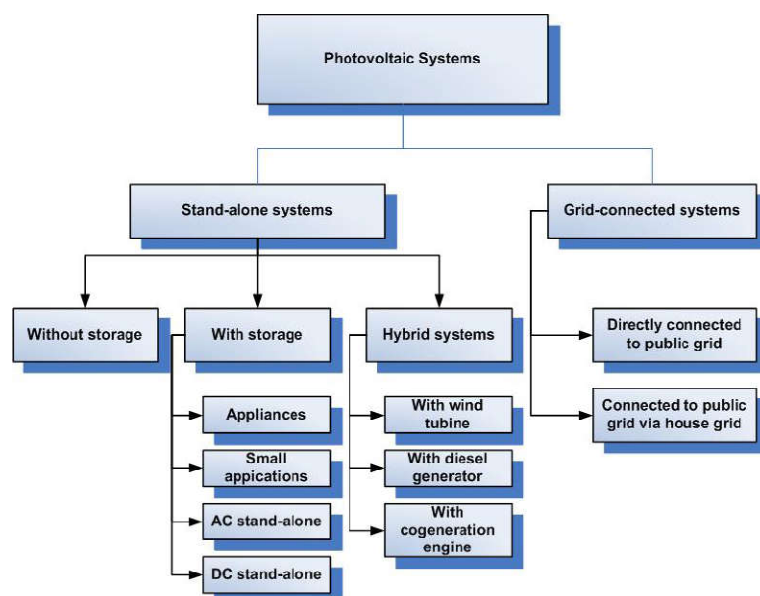


Fig.1.6: Classification of PV systems



### 1.4.1 PV cell

PVs generate electric power when illuminated by sunlight or artificial light. To illustrate the operation of a PV cell the p-n homo junction cell is used. PV cells contain a junction between two different materials across which there is a built in electric field. The absorption of photons of energy greater than the band gap energy of the semiconductor promotes electrons from the valence band to the conduction band, creating hole-electron pairs throughout the illuminated part of the semiconductor. These electron and hole pairs will flow in opposite directions across the junction thereby creating DC power.

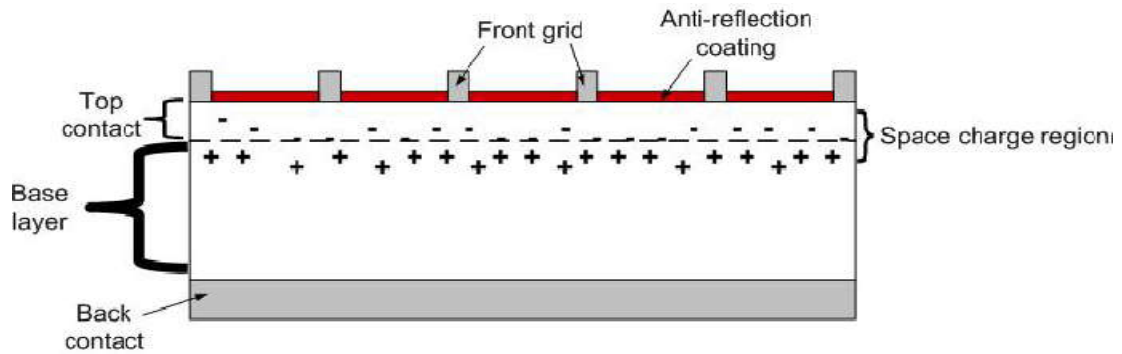


Fig.1.7: Structure of a PV cell

The cross-section of a PV cell is shown in Figure 1.7. The most common material used in PV cell manufacture is mono-crystalline or poly-crystalline silicon. Each cell is typically made of square or rectangular wafers of dimensions measuring about 10cm X10cm X0.3mm. In the dark the PV cell's behavior is similar to that of a diode and the well known Shockley-Read equation can be used to model its behavior i.e.

$$i = I_s \left( e^{\frac{qV}{\beta kT}} - 1 \right)$$

### 1.4.2 PV Module

For the majority of applications multiple solar cells need to be connected in series or in parallel to produce enough voltage and power. Individual cells are usually connected into a series string of cells (typically 36 or 72) to achieve the desired output voltage. The complete assembly is usually referred to as a module and manufacturers basically sell modules to customers. The modules serves another function of protecting

individual cells from water, dust etc. as the solar cells are placed into an encapsulation of single or double at glasses.

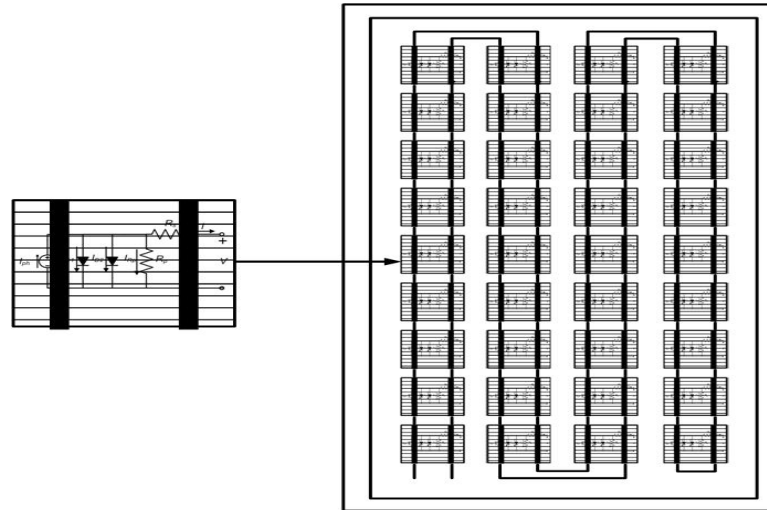


Fig.1.8: Structure of a PV module with 36 cells connected in series

Within a module the different cells are connected electrically in series or in parallel although most modules have a series connection. Figure 1.8 shows a typical connection of how 36 cells are connected in series. In a series connection the same current flows through all the cells and the voltage at the module terminals is the sum of the individual voltages of each cell. It is therefore, very critical for the cells to be well matched in the series string so that all cells operate at the maximum power points. When modules are connected in parallel the current will be the sum of the individual cell currents and the output voltage will equal that of a single cell.

### 1.4.3 Array

An array is a structure that consists of a number of PV modules, mounted on the same plane with electrical connections to provide enough electrical power for a given application. Arrays range in power capacity from a few hundred watts to hundreds of kilowatts. The connection of modules in an array is similar to the connection of cells in a single module. To increase the voltage, modules are connected in series and to increase the current they are connected in parallel. Matching is again very important for the overall performance of the array. The structure of an array is shown in figure 1.9, which has 4 parallel connections of 4 module strings connected in series.

The voltages for  $n$  modules in series are given as:

$$V_{series} = \sum_{j=1}^n V_j = V_1 + V_2 + \dots + V_n \text{ for } I > 0 \quad (1.1)$$

$$V_{seriesoc} = \sum_{j=1}^n V_j = V_{oc1} + V_{oc2} + \dots + V_{ocn} \text{ for } I = 0 \quad (1.2)$$

The current and voltage for m modules in parallel is given

$$I_{parallel} = \sum_{j=1}^n I_j = I_1 + I_2 + \dots + I_n$$

$$V_{parallel} = V_1 = V_2 = \dots = V_n \quad (1.3)$$

For an array to perform well all the modules must not be shaded otherwise it will act as a load resulting in heat that may cause damage. Bypass diodes are usually used to avoid damage although they result in further increase in cost. Integration of bypass diodes in some large modules during manufacturing is not uncommon and reduces the extra wiring required. It must be pointed out though that it becomes very difficult to replace the diode if it fails.

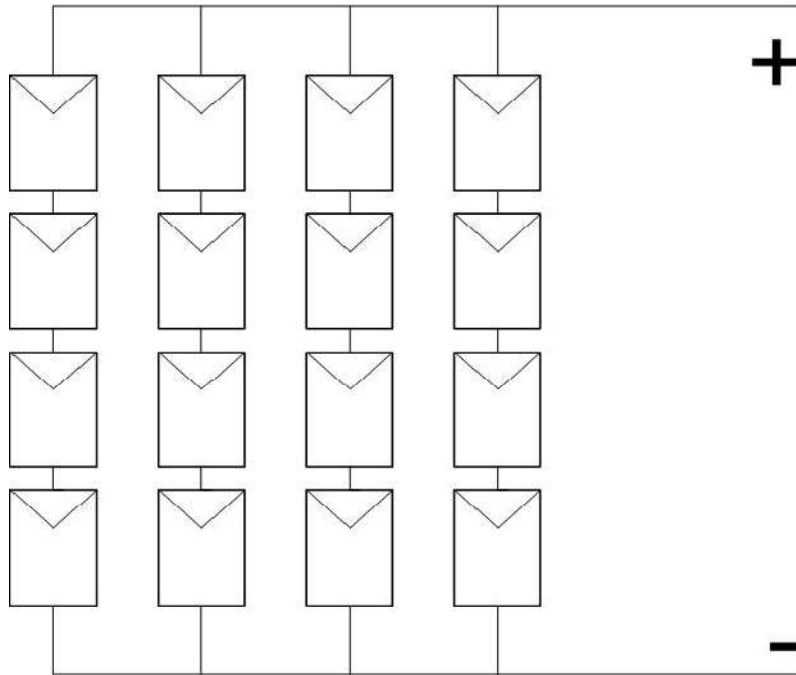


Fig.1.9: Structure of a PV array

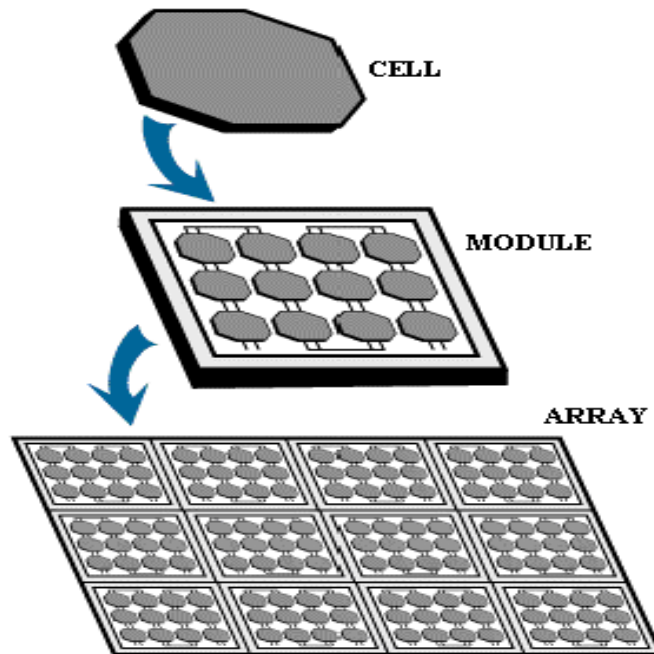


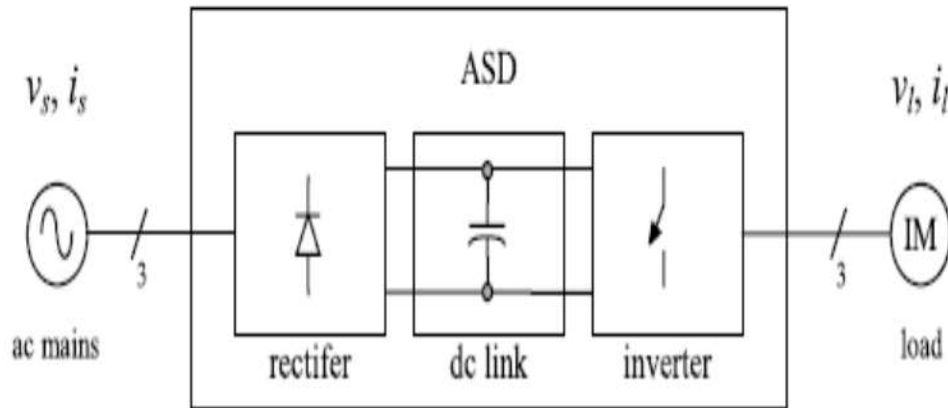
Fig: 1.10 Model of PV cell

## 1.5 VOLTAGE SOURCE INVERTERS

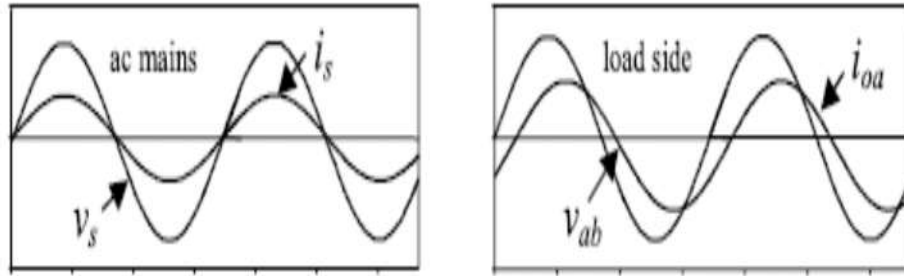
The main objective of static power converters is to produce an ac output waveform from a dc power supply. These are the types of waveforms required in adjustable speed drives (ASDs), uninterruptible power supplies (UPS), static var compensators, active filters, flexible ac transmission systems (FACTS), and voltage compensators, which are only a few applications. For sinusoidal ac outputs, the magnitude, frequency, and phase should be controllable. According to the type of ac output waveform, these topologies can be considered as voltage source inverters (VSIs), where the independently controlled ac output is a voltage waveform. These structures are the most widely used because they naturally behave as voltage sources as required by many industrial applications, such as adjustable speed drives (ASDs), which are the most popular application of inverters. Similarly, these topologies can be found as current source inverters (CSIs), where the independently controlled ac output is a current waveform. These structures are still widely used in medium-voltage industrial applications, where high-quality voltage waveforms are required. Static power converters, specifically inverters, are constructed from power switches and the ac output waveforms are therefore made up of discrete values. This leads to the generation of waveforms that feature fast transitions rather than smooth ones. For instance, the ac

output voltage produced by the VSI of a standard ASD is a three-level waveform (Fig.1.11c). Although this waveform is not sinusoidal as expected (Fig.1.11b), its fundamental component behaves as such. This behavior should be ensured by a modulating technique that controls the amount of time and the sequence used to switch the power valves on and off. The modulating techniques most used are the carrier-based technique (e.g., sinusoidal pulse width modulation, SPWM), the space-vector (SV) technique, and the selective-harmonic elimination (SHE) technique.

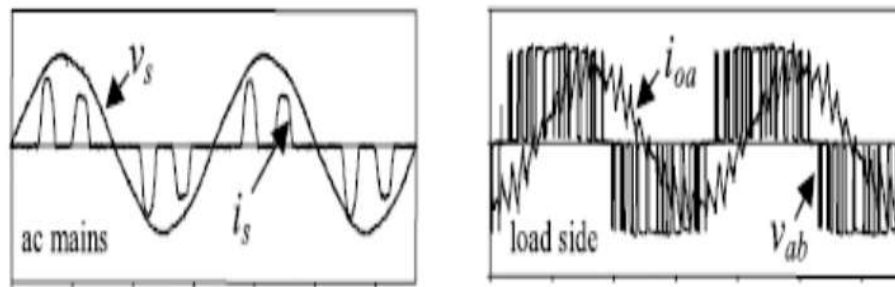
VSI-based controller is to introduce a semiconductor controlled device which is capable of emulating the characteristics of the excitation capacitors and injecting adequate reactive power into the induction generator and the load. The secondary objective is the regulation of the real power. The proposed controller employs a DC side resistor such that the unwanted real power will be consumed in this resistor. As a consequence, the induction generator will always observe a constant real power demand. This VSI-based controller can replace the earlier reported impedance controller and eliminates the need for excitation capacitor. Due to the nature of the VSI-based controller, a wider control range that can accommodate various control operations of the overall system is achievable. The controller is capable of delivering or receiving real and reactive power. This control should be performed in such a way that the real and reactive power components can be controlled independently. Moreover, the VSI-based controller should be able to respond rapidly to the control commands, and drive the operating point of the system to the desired one.



1.11(a) The electrical power conversion topology



1.11 (b) The ideal input (ac mains) and output (load) waveforms



1.11 (c) The actual input (ac mains) and output (load) waveforms

Fig.1.11: The ac output voltage produced by the VSI of a standard ASD

## 1.6 SINGLE-PHASE VOLTAGE SOURCE INVERTERS

Single-phase voltage source inverters (VSIs) can be found as half-bridge and full-bridge topologies. Although the power range they cover is the low one, they are widely used in power supplies, single-phase UPSs, and currently to form elaborate high-power static power topologies, such as for instance, the multicell configurations.

### 1.7 HALF-BRIDGE VSI

Fig.1.12 shows the power topology of a half-bridge VSI, where two large capacitors are required to provide a neutral point N, such that each capacitor maintains a constant voltage  $(V_i)/2$ . Because the current harmonics injected by the operation of the inverter are low-order harmonics, a set of large capacitors ( $C_+$  and  $C_-$ ) is required. It is clear that both switches  $S_+$  and  $S_-$  cannot be ON simultaneously because a short circuit across the dc link voltage source  $V_i$  would be produced. There are two defined (states 1 and 2) and one undefined (state 3) switch state as shown in Table 1.2. In order to avoid the short circuit across the dc bus and the undefined ac output voltage condition, the modulating technique should always ensure that at any instant either the top or the bottom switch of the inverter leg is on.

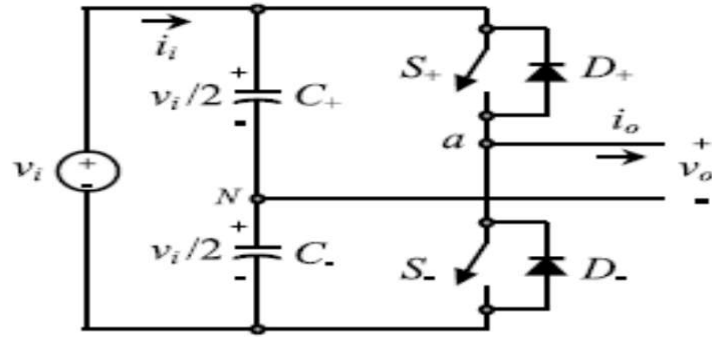


Fig.1.12: Single-phase half-bridge VSI.

State	State	$v$	Components Conducting
$+$ is on and $-$ is off	1	$v/2$	$+$ if $> 0$ $+$ if $< 0$
$-$ is on and $+$ is off	2	$-v/2$	$-$ if $> 0$ $-$ if $< 0$
$+$ and $-$ are all off	3	$-v/2$ $v/2$	$-$ if $> 0$ $+$ if $< 0$

Table 1.2: Switch states for a half-bridge single-phase VSI

### 1.8 FULL-BRIDGE VSI

Fig.1.13 shows the power topology of a full-bridge VSI. This inverter is similar to the half-bridge inverter; however, a second leg provides the neutral point to the load. As expected, both switches  $S_{1+}$  and  $S_{1-}$  (or  $S_{2+}$  and  $S_{2-}$ ) cannot be on simultaneously because a short circuit across the dc link voltage source  $V_i$  would be produced. There are four defined (states 1, 2, 3, and 4) and one undefined (state 5) switch states as shown in Table 1.3. The undefined condition should be avoided so as to be always capable of defining the ac output voltage. It can be observed that the ac output voltage can take values up to the dc link value  $V_i$ , which is twice that obtained with half-bridge VSI topologies. Several modulating techniques have been developed that are applicable to full bridge VSIs. Among them are the PWM (bipolar and unipolar) techniques.

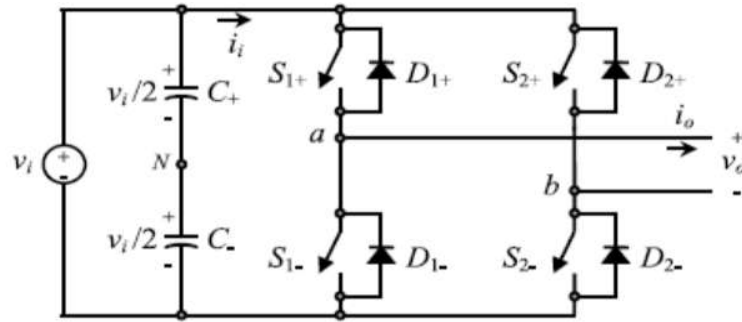


Fig.1.13: Single-phase full-bridge VSI.

State	State	$v_a$	$v_b$	$v$	Components Conducting
$1_+$ and $2_-$ are on and $1_-$ and $2_+$ are off	1	$v/2$	$-v/2$	$v$	$1_+$ and $2_-$ if $> 0$
$1_-$ and $2_+$ are on and $1_+$ and $2_-$ are off	2	$-v/2$	$v/2$	$-v$	$1_+$ and $2_-$ if $< 0$
$1_-$ and $2_+$ are on and $1_+$ and $2_-$ are off	3	$v/2$	$v/2$	0	$1_-$ and $2_+$ if $> 0$
$1_+$ and $2_-$ are on and $1_-$ and $2_+$ are off	4	$-v/2$	$-v/2$	0	$1_-$ and $2_+$ if $< 0$
$1_+$ and $2_-$ are on and $1_-$ and $2_+$ are off	5	$-v/2$	$v/2$	$-v$	$1_+$ and $2_-$ if $> 0$
$1_+$ and $2_-$ are on and $1_-$ and $2_+$ are off		$v/2$	$-v/2$	$v$	$1_+$ and $2_-$ if $< 0$

Table 1.3: Switch states for a full-bridge single-phase VSI

## 1.9 THREE PHASE VOLTAGE SOURCE INVERTERS

Single-phase VSIs cover low-range power applications and three-phase VSIs cover the medium to high-power applications. The main purpose of these topologies is to provide a three-phase voltage source, where the amplitude, phase, and frequency of the voltages should always be controllable. Although most of the applications require sinusoidal voltage waveforms (e.g., ASDs, UPSs, FACTS, VAR compensators), arbitrary voltages are also required in some emerging applications (e.g., active filters, voltage compensators). The standard three-phase VSI topology is shown in Fig.1.14 and the eight valid switch states are given in Table 1.4. As in single-phase VSIs, the switches of any leg of the inverter ( $S_1$  and  $S_4$ ,  $S_3$  and  $S_6$ , or  $S_5$  and  $S_2$ ) cannot be switched on simultaneously because this would result in a short circuit across the dc link voltage supply. Similarly, in order to avoid undefined states in the VSI, and thus undefined ac output line voltages, the switches of any leg of the inverter cannot be switched off simultaneously as this will result in voltages that will depend upon the respective line



current polarity. Of the eight valid states, two of them (7 and 8 in Table 1.4) produce zero ac line voltages. In this case, the ac line currents freewheel through either the upper or lower components. The remaining states (1 to 6 in Table 1.4) produce non-zero ac output voltages. In order to generate a given voltage waveform, the inverter moves from one state to another. Thus the resulting ac output line voltages consist of discrete values of voltages that are  $V_i$ , 0, and  $-V_i$  for the topology shown in Fig.1.14. The selection of the states in order to generate the given waveform is done by the modulating technique that should ensure the use of only the valid states

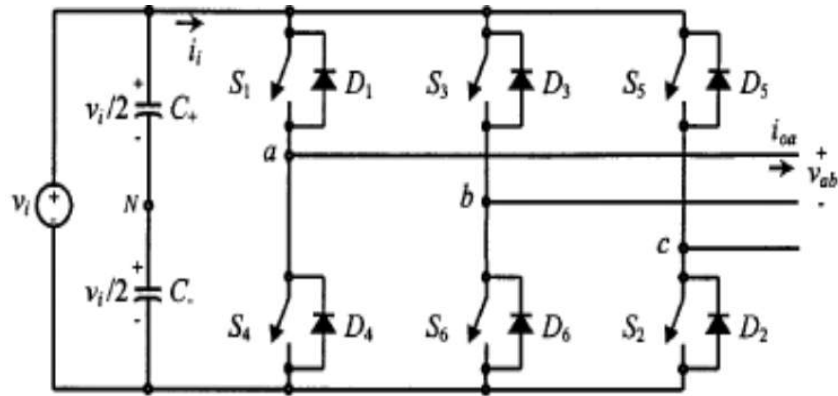


Fig.1.14: Three-phase VSI topology.

State	State	$v_{ab}$	$v_b$	$v_a$	Space Vector
1, 2, and 6 are on and 4, 5, and 3 are off	1	$v$	0	$-v$	$V_1 = 1 + j0.5$
2, 3, and 1 are on and 5, 6, and 4 are off	2	0	$v$	$-v$	$V_2 = j1.155$
3, 4, and 2 are on and 6, 1, and 5 are off	3	$-v$	$v$	0	$V_3 = -1 + j0.5$
4, 5, and 3 are on and 1, 2, and 6 are off	4	$-v$	0	$v$	$V_4 = -1 - j0.5$
5, 6, and 4 are on and 2, 3, and 1 are off	5	0	$-v$	$v$	$V_5 = -j1.155$
6, 1, and 5 are on and 3, 4, and 2 are off	6	$v$	$-v$	0	$V_6 = 1 - j0.5$
1, 3, and 5 are on and 4, 6, and 2 are off	7	0	0	0	$V_7 = 0$
4, 6, and 2 are on and 1, 3, and 5 are off	8	0	0	0	$V_8 = 0$

Table 1.4: Valid switch states for a three-phase VSI

## 1.10 MAXIMUM POWER POINT TRACKING

Maximum power point tracking (MPPT) is a technique used with wind turbines and photovoltaic (PV) solar systems to maximize power output.

This concerns itself primarily with solar photovoltaics, but the basic theory applies to other uses of power photovoltaics such as optical power transmission and thermophotovoltaics. The efficiency of other types of power generation systems (such as wind turbines) can be optimized with similar load optimization concepts, though the form of the I-V curve may differ. It is of greatest interest when the power available to the system is variable, which is commonly the case in solar photovoltaics.

PV solar systems exist in many different configurations with regard to their relationship to inverter systems, external grids, battery banks, or other electrical loads. Regardless of the ultimate destination of the solar power though, the central problem addressed by MPPT is that the efficiency of power transfer from the solar cell depends on both the amount of sunlight falling on the solar panels and the electrical characteristics of the load. As the amount of sunlight varies, the load characteristic that gives the highest power transfer efficiency changes, so that the efficiency of the system is optimized when the load characteristic changes to keep the power transfer at highest efficiency. This load characteristic is called the maximum power point and MPPT is the process of finding this point and keeping the load characteristic there. Electrical circuits can be designed to present arbitrary loads to the photovoltaic cells and then convert the voltage, current, or frequency to suit other devices or systems, and MPPT solves the problem of choosing the best load to be presented to the cells in order to get the most usable power out.

Solar cells have a complex relationship between temperature and total resistance that produces a non-linear output efficiency which can be analyzed based on the I-V curve. It is the purpose of the MPPT system to sample the output of the PV cells and apply the proper resistance (load) to obtain maximum power for any given environmental conditions. MPPT devices are typically integrated into an electric power converter system that provides voltage or current conversion, filtering, and regulation for driving various loads, including power grids, batteries, or motors.

- Solar inverters convert the DC power to AC power and may incorporate MPPT: such inverters sample the output power (I-V curve) from the solar modules and apply the proper resistance (load) so as to obtain maximum power.
- The power at the MPP ( $P_{mpp}$ ) is the product of the MPP voltage ( $V_{mpp}$ ) and MPP current ( $I_{mpp}$ ).

### 1.10.1 I-V curve

Photovoltaic cells have a complex relationship between their operating environment and the maximum power they can produce. The fill factor, abbreviated FF, is a parameter which characterizes the non-linear electrical behavior of the solar cell. Fill factor is defined as the ratio of the maximum power from the solar cell to the product of Open Circuit Voltage  $V_{oc}$  and Short-Circuit Current  $I_{sc}$ . In tabulated data it is often used to estimate the maximum power that a cell can provide with an optimal load under given conditions,  $P = FF \cdot V_{oc} \cdot I_{sc}$ . For most purposes, FF,  $V_{oc}$ , and  $I_{sc}$  are enough information to give a useful approximate model of the electrical behavior of a photovoltaic cell under typical conditions.

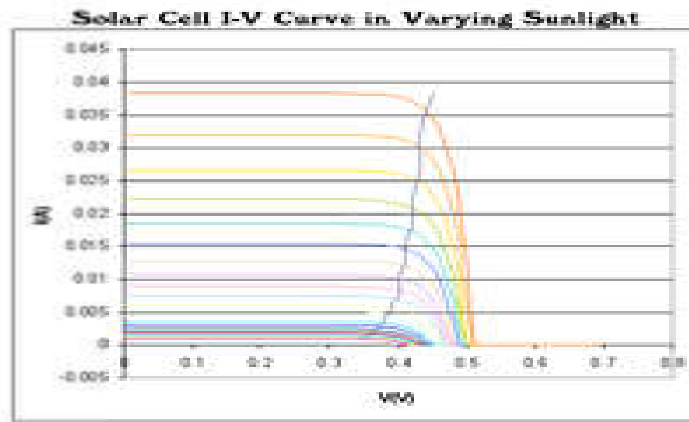


Fig.1.15 Photovoltaic solar cell I-V curves where a line intersects the knee of the curves where the maximum power transfer point is located.

For any given set of operational conditions, cells have a single operating point where the values of the current ( $I$ ) and Voltage ( $V$ ) of the cell result in a maximum power output. These values correspond to a particular load resistance, which is equal to  $V / I$  as specified by Ohm's Law. The power  $P$  is given by  $P = V \cdot I$ . A photovoltaic cell, for the majority of its useful curve, acts as a constant current source. However, at a photovoltaic cell's MPP region, its curve has an approximately inverse exponential relationship between current and voltage. From basic circuit theory, the power delivered from or to a device is optimized where the derivative (graphically, the slope)  $dI/dV$  of the I-V curve is equal and opposite the  $I/V$  ratio (where  $dP/dV = 0$ ). This is known as the maximum power point (MPP) and corresponds to the "knee" of the curve.

A load with resistance  $R=V/I$  equal to the reciprocal of this value draws the maximum power from the device. This is sometimes called the 'characteristic resistance' of the cell. This is a dynamic quantity which changes depending on the level of illumination, as well as other factors such as temperature and the age of the cell. If the resistance is lower or higher than this value, the power drawn will be less than the maximum available, and thus the cell will not be used as efficiently as it could be. Maximum power point trackers utilize different types of control circuit or logic to search for this point and thus to allow the converter circuit to extract the maximum power available from a cell.

### 1.11 CLASSIFICATION

Controllers can follow several strategies to optimize the power output of an array. Maximum power point trackers may implement different algorithms and switch between them based on the operating conditions of the array.

#### 1.11.1 Perturb and observe

In this method the controller adjusts the voltage by a small amount from the array and measures power; if the power increases, further adjustments in that direction are tried until power no longer increases. This is called the perturb and observe method and is most common, although this method can result in oscillations of power output. It is referred to as a hill climbing method, because it depends on the rise of the curve of power against voltage below the maximum power point, and the fall above that point. Perturb and observe is the most commonly used MPPT method due to its ease of implementation. Perturb and observe method may result in top-level efficiency, provided that a proper predictive and adaptive hill climbing strategy is adopted.

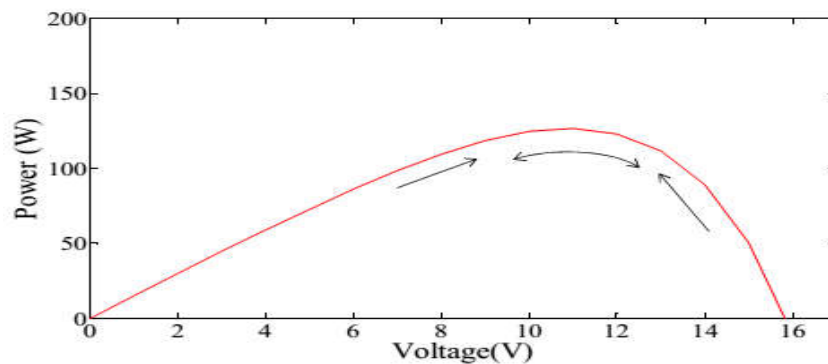


Fig.1.16. Perturb and observe algorithm

The algorithm observes output power of the array and perturbs the power based on increment of the array voltage. The algorithm continuously increments or decrements the reference voltage based on the value of the previous power sample.

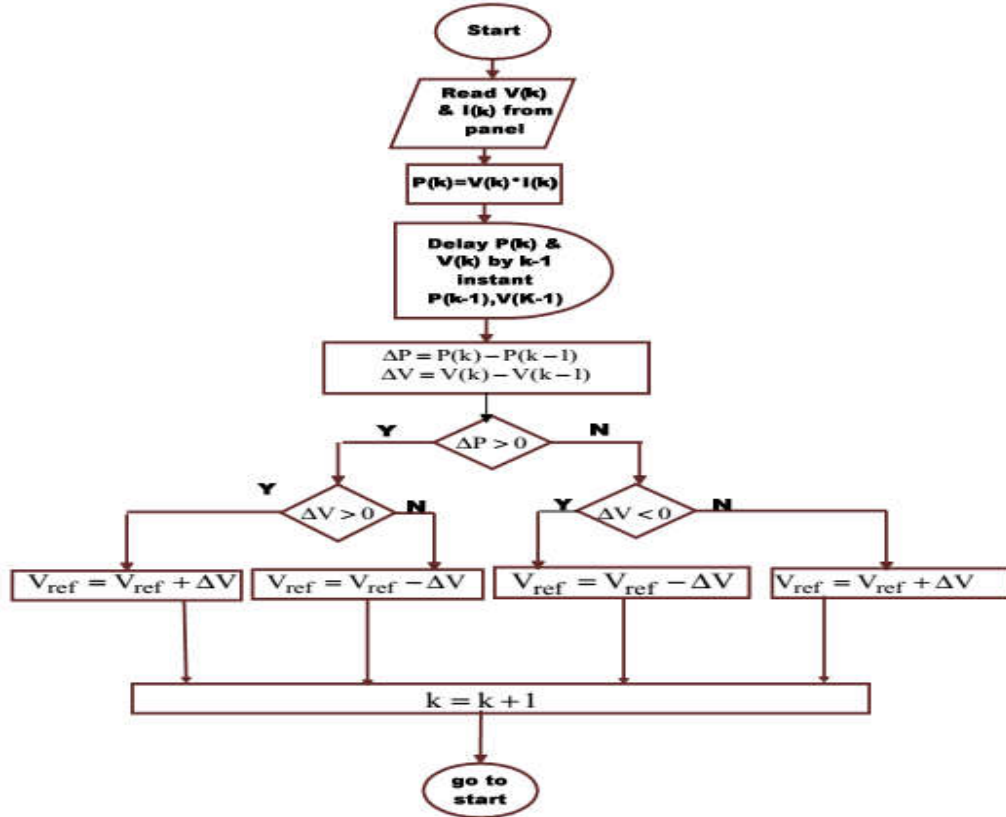


Fig.1.17. Flowchart Perturb and observe algorithm

### 1.11.2 Incremental conductance

In the incremental conductance method, the controller measures incremental changes in PV array current and voltage to predict the effect of a voltage change. This method requires more computation in the controller, but can track changing conditions more rapidly than the perturb and observe method (P&O). Like the P&O algorithm, it can produce oscillations in power output. This method utilizes the incremental conductance ( $dI/dV$ ) of the photovoltaic array to compute the sign of the change in power with respect to voltage ( $dP/dV$ ).

The incremental conductance method computes the maximum power point by comparison of the incremental conductance ( $I_{\Delta} / V_{\Delta}$ ) to the array conductance ( $I / V$ ).

When these two are the same ( $I / V = I_{\Delta} / V_{\Delta}$ ), the output voltage is the MPP voltage. The controller maintains this voltage until the irradiation changes and the process is repeated.

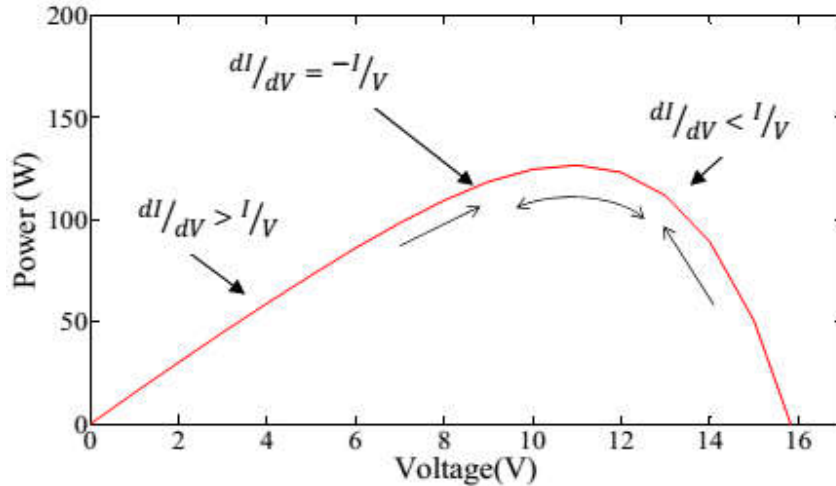


Fig.1.18. Incremental conductance algorithm

### 1.11.3 Current sweep

The current sweep method uses a sweep waveform for the PV array current such that the I-V characteristic of the PV array is obtained and updated at fixed time intervals. The maximum power point voltage can then be computed from the characteristic curve at the same intervals.

### 1.11.4 Constant voltage

The term "constant voltage" in MPP tracking is used to describe different techniques by different authors, one in which the output voltage is regulated to a constant value under all conditions and one in which the output voltage is regulated based on a constant ratio to the measured open circuit voltage (VOC). The latter technique is referred to in contrast as the "open voltage" method by some authors. If the output voltage is held constant, there is no attempt to track the maximum power point, so it is not a maximum power point tracking technique in a strict sense, though it does have some advantages in cases when the MPP tracking tends to fail, and thus it is sometimes used to supplement an MPPT method in those cases.

In the "constant voltage" MPPT method (also known as the "open voltage method"), the power delivered to the load is momentarily interrupted and the open-circuit voltage with zero current is measured. The controller then resumes operation with the voltage controlled at a fixed ratio, such as 0.76, of the open-circuit voltage VOC. This is

usually a value which has been determined to be the maximum power point, either empirically or based on modelling, for expected operating conditions. The operating point of the PV array is thus kept near the MPP by regulating the array voltage and matching it to the fixed reference voltage  $V_{ref}=kV_{OC}$ . The value of  $V_{ref}$  may be also chosen to give optimal performance relative to other factors as well as the MPP, but the central idea in this technique is that  $V_{ref}$  is determined as a ratio to  $V_{OC}$ .

One of the inherent approximations to the "constant voltage" ratio method is that the ratio of the MPP voltage to  $V_{OC}$  is only approximately constant, so it leaves room for further possible optimization.

#### **1.11.5 Comparison of methods**

Both perturb and observe, and incremental conductance, are examples of "hill climbing" methods that can find the local maximum of the power curve for the operating condition of the PV array, and so provide a true maximum power point.

The perturb and observe method requires oscillating power output around the maximum power point even under steady state irradiance.

The incremental conductance method has the advantage over the perturb and observe (P&O) method that it can determine the maximum power point without oscillating around this value. It can perform maximum power point tracking under rapidly varying irradiation conditions with higher accuracy than the perturb and observe method. However, the incremental conductance method can produce oscillations (unintentionally) and can perform erratically under rapidly changing atmospheric conditions. The sampling frequency is decreased due to the higher complexity of the algorithm compared to the P&O method.

In the constant voltage ratio (or "open voltage") method, the current from the photovoltaic array must be set to zero momentarily to measure the open circuit voltage and then afterwards set to a predetermined percentage of the measured voltage, usually around 76%. Energy may be wasted during the time the current is set to zero. The approximation of 76% as the MPP/ $V_{OC}$  ratio is not necessarily accurate though. Although simple and low-cost to implement, the interruptions reduce array efficiency and do not ensure finding the actual maximum power point. However, efficiencies of some systems may reach above 95%.

### **1.11.6 MPPT placement**

Traditional solar inverters perform MPPT for the entire PV array (module association) as a whole. In such systems the same current, dictated by the inverter, flows through all modules in the string (series). Because different modules have different I-V curves and different MPPs (due to manufacturing tolerance, partial shading, etc.) this architecture means some modules will be performing below their MPP, resulting in lower efficiency.

Some companies (see power optimizer) are now placing maximum power point tracker into individual modules, allowing each to operate at peak efficiency despite uneven shading, soiling or electrical mismatch.

Data suggests having one inverter with one MPPT for a project that has east and west-facing modules presents no disadvantages when compared to having two inverters or one inverter with more than one MPPT.

### **1.11.7 Operation with batteries**

At night, an off-grid PV system may use batteries to supply loads. Although the fully charged battery pack voltage may be close to the PV panel's maximum power point voltage, this is unlikely to be true at sunrise when the battery has been partially discharged. Charging may begin at a voltage considerably below the PV panel maximum power point voltage, and an MPPT can resolve this mismatch.

When the batteries in an off-grid system are fully charged and PV production exceeds local loads, an MPPT can no longer operate the panel at its maximum power point as the excess power has no load to absorb it. The MPPT must then shift the PV panel operating point away from the peak power point until production exactly matches demand. (An alternative approach commonly used in spacecraft is to divert surplus PV power into a resistive load, allowing the panel to operate continuously at its peak power point.)

In a grid connected photovoltaic system, all delivered power from solar modules will be sent to the grid. Therefore, the MPPT in a grid connected PV system will always attempt to operate the PV modules at its maximum power point.

### **1.12 Water Pumps**

The two broad categories of pumps are generally used for PV powered pumping systems: centrifugal and volumetric (displacement) pumps.



### 1.12.1 Centrifugal Pumps

Centrifugal pumps have a rotating impeller that throws the water radially against a casing so shaped that the momentum of the water is converted into useful pressure for lifting. They are normally used for low head / low pressure applications, particularly if direct connection to the solar panels is required. They are well suited to high pumping rates and due to their compactness; wherever small diameter bores or well exists. Centrifugal pumps are characterized by the torque being proportional to the square of the speed (angular velocity of the impeller).

These pumps have relatively high efficiencies, but rapidly lose pumping performances as their speed reduces and in fact do not pump at all unless quite substantial spin speeds are achieved. This is a problem for a PV powered system when light intensity is reduced. Maximum speed performance is achieved at high spin speeds, making them easy to match to motors, which tend to develop maximum torque (maximum efficiency) at similar speeds.

For conventional centrifugal pump designs, high efficiencies are only obtained for low pumping pressures and hence relatively small pumping heads of less than 25 meters. To overcome this limitation, either multistage or regenerative centrifugal pumps can be used.

Other advantages of centrifugal pumps include their simplicity (with a minimum of moving parts) and corresponding reliability, low cost, robustness, tolerance to pumping particulates and low starting torque. On the other hand, another potential limitation of centrifugal pumps is their inability to be self-priming. Consequently, they are frequently used as submersible pumps, preferably in conjunction with a submersible motor. Alternatively, self-priming centrifugal pumps where a chamber containing water at the side of the pump keeps the pump effectively submerged and hence primed is also used.

The major trade-off involved with the design and use of centrifugal pumps is the requirement for high efficiency versus the need for an impeller with long life and good tolerance of aggressive impurities in the water. High efficiency can be obtained with small clearances and narrow passages, but this is undesirable for pump reliability and the ability to pump liquids contaminated with particles. In addition, high efficiency can be obtained

with a high speed impeller which again acts to shorten the life of the pump. In summary, pumps need to be designed and selected for specific application and environments.

### 1.12.2 Volumetric Pumps

Volumetric or positive displacement pumps are the other class of pumps often used for water pumping applications, particularly for lower pump rates from deep wells or bores. Examples of volumetric or positive displacement pumps are peristaltic pumps, diaphragm pumps, rotary-screw type pumps and progressive cavity pumps.

### 1.13 ZETA CONVERTER

A zeta converter is a fourth order non linear system being that, with regard to energy input, it can be seen as buck-boost-buck converter and with regard to the output, it can be seen as boost-buck-boost converter.

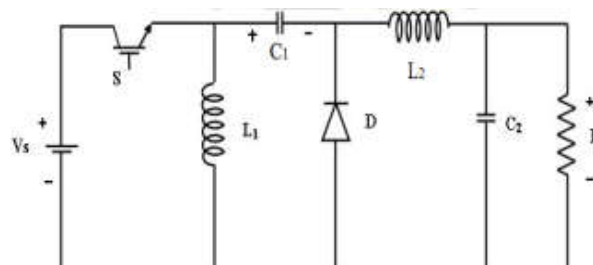


Fig.1.19 Basic Zeta converter circuit

The ideal switch based realization of zeta converter is depicted. A non-isolated zeta converter circuit is shown in the fig.1.14 above. Although several operating modes are possible for this converter depending on inductance value, load resistance and operating frequency, here only continuous inductor current,  $i_{L1}$  is analyzed using the well known state-space averaging method.

The analysis uses the following assumptions.

1. Semiconductors switching devices are considered to be ideal.
2. Converter operating in continuous inductor current mode.
3. Line frequency ripple in the dc voltage is neglected.

#### 1.13.1 Modes of Operation

Zeta converter exhibits two different modes as follows:

**Mode1:** The first mode is obtained when the switch is ON (closed) and instantaneously, the diode D is OFF. An equivalent circuit shown in Fig.1.20. During this period, the

current through the inductor  $L_1$  and  $L_2$  are drawn from the voltage source  $V_s$ . This mode is the **charging** mode

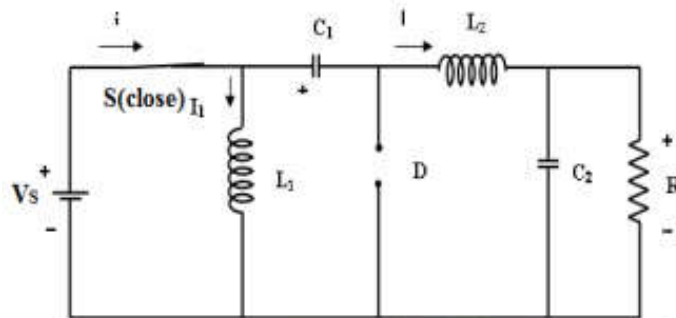


Fig.1.20 Equivalent circuit of converter (switch ON)

**Mode2:** The second mode of operation starts when the switch is OFF and the diode  $D$  is ON position, the equivalent circuit shown in Fig.1.21. This stage or mode of operation is known as the **discharging** mode since all the energy stored in  $L_2$  is now transferred to the load  $R$ .

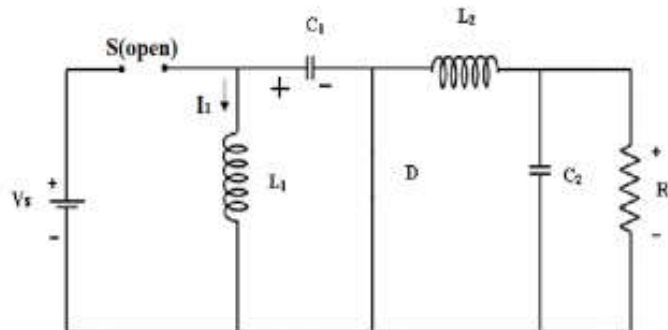


Fig.1.21 Equivalent circuit of converter (switch OFF)

## **CHAPTER 2**

### **LITERATURE SURVEY**

#### **2.1 DC-to-DC Converter with Low Input Current Ripple for Maximum Photovoltaic Power Extraction [11]**

Owing to the need for maximum utilization of solar cells, fuel cells, wind turbines, and batteries, dc-to-dc converters with continuous input energy flow are widely used for renewable energy applications. To save energy, rather than converting to another energy form, the photovoltaic (PV) source output current and voltage should be continuous (and nonzero) for maximum renewable energy extraction. Also, the dc-to-dc converters must assure continuous input and output current to provide maximum energy flow from the source to the load. Therefore, an LC filter, a large capacitor, or a continuous current converter can be adopted for continuous PV output energy. Adding either an LC or a C filter can create electrical resonance issues, costs money, increases weight and volume, plus decreases reliability, particularly in the case of electrolytic capacitors. In avoiding these issues, the PV must draw continuous current to provide better maximum power point tracking (MPPT) with minimal energy ripple.

Power supplies employ electrolytic capacitors for energy storage and to reduce input current and output voltage ripple. Although electrolytic capacitance can be large, such capacitors have a short lifetime owing to the liquid electrolyte, thus restricting performance enhancement of a long lifetime system. The lifetime of the electrolytic capacitor is limited to a few thousand hours at rated operating conditions, which are shorter than the lifetime of other components like light-emitting diodes (LEDs), lead-acid batteries, and PV panels. Hence, the electrolytic capacitor is an obstacle to the overall reliability of PV systems and thus is significantly derated. The lifetime may only be 1000 h at rated conditions, as every 10°C decrease in operating temperature doubles the lifetime. The LED lifetime is generally higher than 80 000 h, while the lead-acid battery lifetime reaches ten years and additionally is recyclable.

The current ripple creates a problem in power electronics systems, which affects the voltage and, thus, the power. The extent of the loss problem due to PV current ripple is a feature realized for the first time in this paper. The exponential curve of the PV cells

causes nonlinear mapping in the current axis which, in turn, leads to the high loss of output power due to the input current ripple. With current ripple, the controller, which will have a bandwidth less than the converter switching frequency, does not operate around the dc MPP. Rather, the average point is changed when extracting maximum power. As the PV current ripple decreases, the average operating point converges to the PV dc operating MPP. The assessment of converter interfacing for PV sources has underlying decoupling capacitance requirements to operate at maximum power with minimal ripple, with large capacitance filtering needed for converters with discontinuous input current.

The actual power losses are considerably larger than that expected from modest small-signal approaches. The higher drop in power is clarified and experimentally established in the authors establish that the 8% ripple rms amplitude of the MPP voltage results in a 5% drop in the PV power output which is 5% of the PV efficiency. Under nonuniform irradiance, this percentage loss can be significantly higher, and such results are confirmed in this paper. The authors consider sensitivity to ripple in voltage and current at the terminals of the PV module. Their simulations verify a power loss of 1% when the amplitude of the ripple voltage is equal to 6% of the MPP voltage, and a loss of 2% for an 8.5% voltage ripple. Such effects have not been studied extensively in the literature, particularly the effects of the current ripple on the PV module, in terms of MPPT design or ripple from the dc-to-dc converter. The losses reach 5%, while in the losses reach 2% of the PV efficiency at around 8% ripple of the MPP voltage. This is because many factors affect the percentage loss, such as irradiance level, fill factor of the PV module, and nonuniform weather conditions. In this paper, as established in previous studies, the higher the irradiance level, the lower the effect of the current ripple, or the lower the irradiance level, the greater the effect of the current ripple and hence the lower the PV efficiency.

### **2.1.1 Effect of Input Current Ripple**

Current ripple refers to the variations of the dc component met in switching mode power supplies (SMPSs). Input current ripple from SMPS encloses harmonics, requiring appropriatedesign to decrease or eliminate the ripple. Some concepts concerning the effect of the current ripple are discussed. Filtering is usually used to accomplish low current ripple, which commonly employs bulky reactive components to guarantee the

significant harmonic suppression of low-order components. Utilizing bulky filters, nevertheless, is not an economic solution for SMPS.

The notion of zero input current ripple of SMPS is not new. It is utilized to maximize the power density of the converter and consequently is of significant concern in SMPS. Two motives make it essential to eliminate the input current ripple. First, it decreases the capacitor stress, resulting in either small losses or a stress-free filter. Second, it reduces the noise accompanied to the load, where the pulsating current affects most converters' output and input.

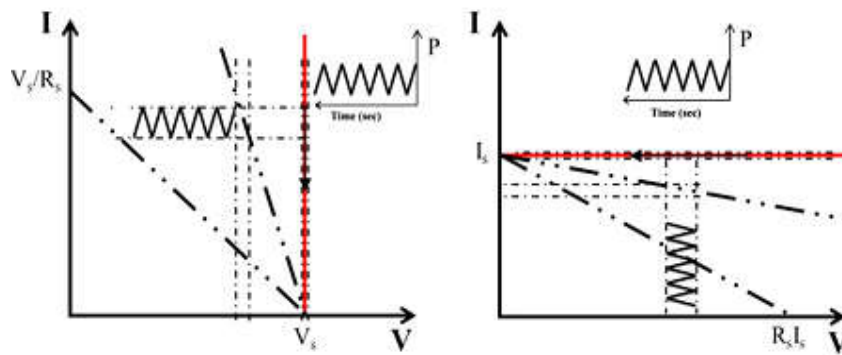


Fig.2.1. Effect of the input current ripple on the dc power supply.

Moreover, current ripple has a notable impact when connected to a solar panel. In Fig.2.1, both ideal current and voltage sources do not produce any ripple. Usually, voltage and current power supplies are not ideal, and the input resistance reflects insignificant ripple on the voltage and current curves. The solar panel works as a current or voltage source and can also be counted as both a voltage and a current source. Fig.2.2 clarifies the impact of the current ripple on the power curve, whence considerable PV power is dropped off because of the curve knee. Unluckily, the characteristics of the solar panel vary according to the temperature and radiation, which maximize the losses. As current ripple increases, the operating point moves to the constant voltage region of the solar panel characteristic, which causes a severe drop in the average power. Therefore, the algorithms based on maximum average power are not MPP trackers. By increasing the average power, the operating point's mean moves to the MPP as the current ripple decreases to zero.

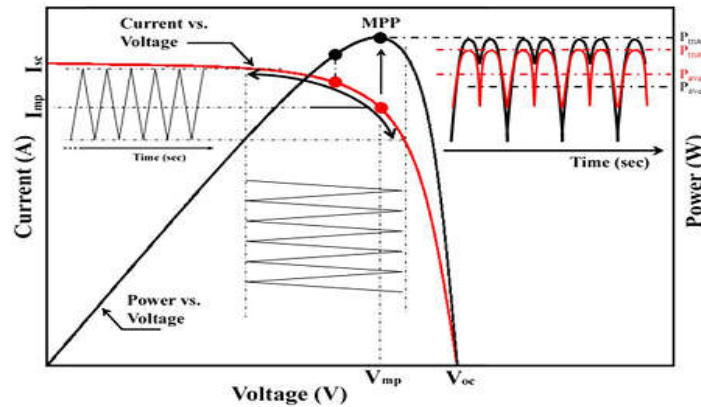


Fig.2.2. Effect of input current ripple on the PV power curve

If current ripple exists, the MPP algorithm cannot achieve the maximum power. For zero input current ripple, the maximum power can be accomplished since the MPP can be tracked.

## 2.2 A Comparative Study on Maximum Power Point Tracking Techniques for Photovoltaic Power Systems [16]

Due to the growing demand on electricity, the limited stock and rising prices of conventional sources (such as coal and petroleum, etc.), photovoltaic (PV) energy becomes a promising alternative as it is omnipresent, freely available, environment friendly, and has less operational and maintenance costs. Therefore, the demand of PV generation systems seems to be increased for both standalone and grid-connected modes of PV systems. Therefore, an efficient maximum power point tracking (MPPT) technique is necessary that is expected to track the MPP at all environmental conditions and then force the PV system to operate at that MPP point. MPPT is an essential component of PV systems. Several MPPT techniques together with their implementation are reported in the literature. Users always feel confused while selecting an MPPT technique for a particular application. Unfortunately, only a few papers are available in this field that includes discussions on MPPT techniques until 2007. But many new MPPT techniques such as distributed MPPT, the Gauss-Newton technique, adaptive perturbation and observation, estimated perturbation and perturb, adaptive fuzzy and particle swarm optimization (PSO)-based MPPT, etc., have been reported since then. Hence, it is necessary to prepare a review that includes all the efficient and effective MPPT techniques proposed before 2007 and after that until 2012. In this review, an attempt has also been made to compare

the MPPT techniques on the basis of their advantages, disadvantages, control variables involved, types of circuitry, complexity of algorithm, complexity level on hardware implementation, and types of scientific and commercial application. This paper attempts to provide a comparative review on most of the reported MPPT techniques excluding any unintentionally omitted papers because of space limitations.

### 2.2.1 Review on MPPT Techniques

The following techniques are some of the widely used MPPT techniques applied on various PV applications such as space satellite, solar vehicles, and solar water pumping, etc.

#### ➤ Curve-Fitting Technique

MPP is the extreme value of the P–V characteristic of a PV panel, hence at first the P–V characteristic of a PV panel is predicted in this technique. To predict, this P–V characteristic, PV panel can be modeled offline based on mathematical equations or numerical approximations.

#### ➤ Fractional Short-Circuit Current (FSCI) Technique

There exists a single operating point P ( $V_{mpp}$ ,  $I_{mpp}$ ) called MPP at which the power of the panel is maximum ( $P_{mpp}$ ) at a given environmental condition (Fig.2.3). If by some means, anyone of  $I_{mpp}$  or  $V_{mpp}$  are tracked then the corresponding  $P_{mpp}$  can be tracked. In the FSCI technique, the nonlinear – characteristics of PV system are modeled using mathematical equations or numerical approximations taking account of a wider range of environmental conditions and degradation level of PV panel.

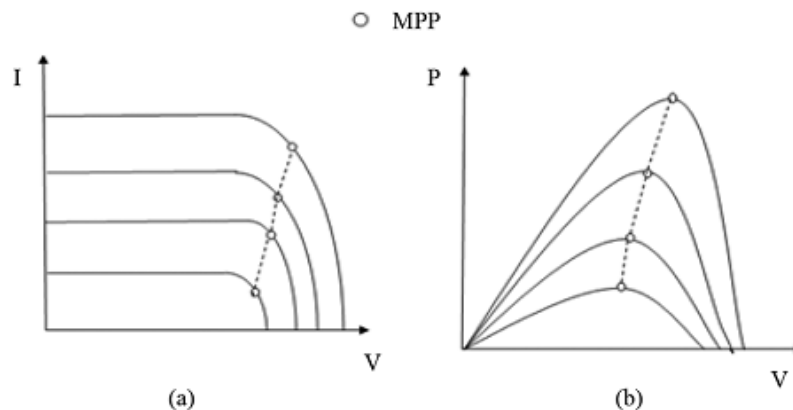


Fig.2.3 (a) I–V and (b) P–V characteristics of PV panel at different environmental conditions.



➤ **Look-up Table Technique**

In this technique, MPP of a PV system is calculated beforehand for each probable environmental condition and stored in the memory device of MPPT's control system. During the operation, the corresponding MPP for a particular condition is selected from that memory and implemented

➤ **One-Cycle Control (OCC) Technique**

OCC is a nonlinear MPPT control technique. It involves the use of a single-stage inverter where the output current ( $I_{out}$ ) of the inverter can be adjusted according to the voltage of the PV array ( $V$ ) so as to extract the maximum power from it. There is only one power conversion stage that realizes on both MPPT control and dc/ac inversion. The OCC system is shown in Fig.2.4. The parameters ( $L, C$ ) involved in this system should be properly tuned as their values greatly affect the accuracy of OCC technique.

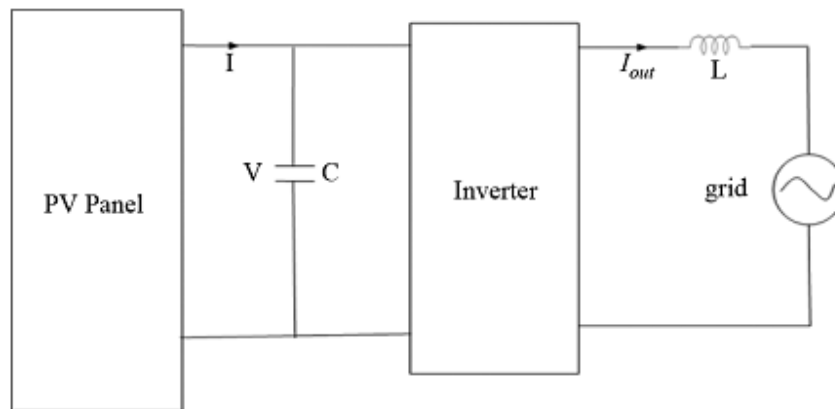


Fig.2.4. Block diagram of OCC technique.

### 2.3 Evaluation of the Main MPPT Techniques for Photovoltaic Applications [17]

The growing energy demand coupled with the possibility of reduced supply of conventional fuels, evidenced by the petroleum crisis, along with growing concerns about environmental conservation, has driven research and development of alternative energy sources that are cleaner, are renewable, and produce little environmental impact. Among the alternative sources, the electrical energy from photovoltaic (PV) cells is currently regarded as a natural energy source that is more useful, since it is free, abundant, clean, and distributed over the Earth and participates as a primary factor of all other processes of energy production on Earth. Moreover, in spite of the phenomena of reflection and absorption of sunlight by the atmosphere, it is estimated that solar energy incident on

the Earth's surface is on the order of ten thousand times greater than the world energy consumption. A great advantage of PV cells is the reduction of carbon dioxide emissions. By the year 2030, the annual reduction rate of CO<sub>2</sub> due to the usage of PV cells may be around 1 Gton/year, which is equivalent to India's total emissions in 2004 or the emission of 300 coal plants. According to experts, the energy obtained from PV cells will become the most important alternative renewable energy source until 2040. In this context, the concept of distributed energy generation became a real and present technical possibility, promoting various research works and standardizations in the world. Despite all the advantages presented by the generation of energy through PV cells, the efficiency of energy conversion is currently low, and the initial cost for its implementation is still considered high; thus, it becomes necessary to use techniques to extract the maximum power from these panels, in order to achieve maximum efficiency in operation. Under uniform solar irradiation conditions, PV panels exhibit a unique operating point where PV power is maximized. The PV power characteristic is nonlinear, as shown in Fig. 2.5 — considering a single PV cell, which varies with the level of solar irradiation and temperature, which make the extraction of maximum power a complex task, considering load variations. Thus, in order to overcome this problem, several methods for extracting the maximum power have been proposed in the literature, and a careful comparison of these methods can result in important information for the design of these systems. Therefore, this paper aims to assess the main maximum power point (MPP) tracking (MPPT) techniques through models in MatLab/Simulink and experimental results, doing depth comparisons among them with regard to the voltage ripple, start-up of the method, tracking factor (TF), and usage of sensors. It should be informed that other papers related to comparisons of MPPT algorithms can be found in the literature. However, this paper presents additional comparisons about the MPPT algorithms, their flowcharts, more interesting experimental results, and the improved modified MPPT proportional–integral (PI)-based IC and perturb and observe (P&O) methods, which presented outstanding performances because of their inherent adaptive capabilities. Finally, experimental results with typical daily power profile are not found in the literature for so many MPPT methods.

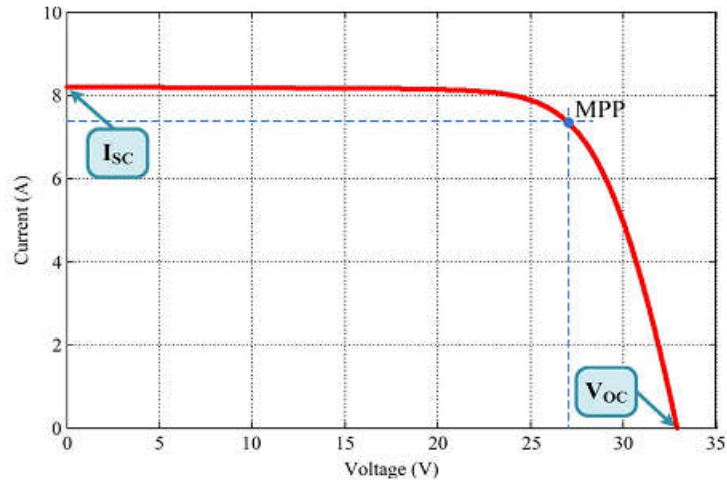


Fig.2.5. PV current-versus-voltage characteristic.

#### ➤ P&O and P&O Based on PI

The P&O method operates by periodically incrementing or decrementing the output terminal voltage of the PV cell and comparing the power obtained in the current cycle with the power of the previous one (performs  $dP/dV$ ). If the voltage varies and the power increases, the control system changes the operating point in that direction; otherwise, it changes the operating point in the opposite direction. Once the direction for the change of voltage is known, the voltage is varied at a constant rate. This rate is a parameter that should be adjusted to allow the balance between faster response and less fluctuation in steady state. A modified version is obtained when the steps are changed according to the distance of the MPP, resulting in higher efficiency. This is an excellent method to reach the MPP, and it is independent from the PV panel/manufacturer; however, this method may suffer from fast changes in environmental conditions.

#### ➤ MPP Locus Characterization

The basic idea of this method is to find a linear relationship between voltage and current at the MPP (MPP locus). This relationship is the tangent line to the MPP locus curve for the PV current in which the minimum irradiation condition satisfies the sensitivity of the method. The equation that guides this method is given. It should be informed that the mathematical derivation is found. As one can observe, it is hard to obtain all the necessary parameters, and a linear approximation is made offline with the PV panel, translating it as an estimation method. As the MPP locus varies with temperature, the model needs to be updated. This is done by measuring the open-circuit voltage

periodically, which means that the interface converter must open the PV circuit, resulting in loss of power in these instants. This MPPT method works better for high solar irradiations.

➤ **CV Method**

The constant voltage (CV) method uses empirical results, indicating that the voltage at MPP ( $V_{MPP}$ ) is around 70%–80% of the PV open-circuit voltage ( $V_{OC}$ ), for the standard atmospheric condition. Among the points of MPP (varying atmospheric conditions), the voltage at the terminals of the module varies very little even when the intensity of solar radiation changes, but it varies when the temperature changes. So, this method must be used in regions where the temperature varies very little. A positive point is that only the PV voltage is necessary to be measured, and a simple control loop can reach the MPP.

## **CHAPTER 3**

### **PROPOSED CONCEPT**

#### **3.1 INTRODUCTION**

The drastic reduction in the cost of power electronic devices and annihilation of fossil fuels in near future invite to use the solar photovoltaic (SPV) generated electrical energy for various applications as far as possible. The water pumping, a standalone application of the SPV array-generated electricity, is receiving wide attention nowadays for irrigation in the fields, household applications, and industrial use. Although several researches have been carried out in an area of SPV array-fed water pumping, combining various dc–dc converters and motor drives, the zeta converter in association with a permanent-magnet brushless dc (BLDC) motor is not explored precisely so far to develop such kind of system. However, the zeta converter has been used in some other SPV-based applications [1]–[3]. Moreover, a topology of SPV array-fed BLDC motor-driven water pump with zeta converter has been reported and its significance has been presented more or less in [4].

Nonetheless, an experimental validation is missing and the absence of extensive literature review and comparison with the existing topologies has concealed the technical contribution and originality of the reported work.

The merits of both BLDC motor and zeta converter can contribute to develop an SPV array-fed water pumping system possessing a potential of operating satisfactorily under dynamically changing atmospheric conditions. The BLDC motor has high reliability, high efficiency, high torque/inertia ratio, improved cooling, low radio frequency interference, and noise and requires practically no maintenance [5], [6]. On the other hand, a zeta converter exhibits the following advantages over the conventional buck, boost, buck–boost converters, and Cuk converter when employed in SPV-based applications.

- 1) Belonging to a family of buck–boost converters, the zeta converter may be operated either to increase or to decrease the output voltage. This property offers a boundless region for maximum power-point tracking (MPPT) of an SPV array [7]. The MPPT can

be performed with simple buck [8] and boost [9] converter if MPP occurs within prescribed limits.

2) This property also facilitates the soft starting of BLDC motor unlike a boost converter which habitually steps up the voltage level at its output, not ensuring soft starting.

3) Unlike a classical buck–boost converter [10], the zeta converter has a continuous output current. The output inductor makes the current continuous and ripples free.

4) Although consisting of same number of components as a Cuk converter [11], the zeta converter operates as non-inverting buck–boost converter unlike an inverting buck–boost and Cuk converter. This property obviates a requirement of associated circuits for negative voltage sensing, and hence reduces the complexity and probability of slowdown the system response [12].

These merits of the zeta converter are favorable for proposed SPV array-fed water pumping system. An incremental conductance maximum power point tracking (INC-MPPT) algorithm [8], [13]–[18] is used to operate the zeta converter such that SPV array always operates at its MPP.

The existing literature exploring SPV array-based BLDC motor-driven water pump [19]–[22] is based on a configuration shown in Fig.3.1. A dc–dc converter is used for MPPT of an SPV array as usual. Two phase currents are sensed along with Hall signals feedback for control of BLDC motor, resulting in an increased cost. The additional control scheme causes increased cost and complexity, which is required to control the speed of BLDC motor. Moreover, usually a voltage-source inverter (VSI) is operated with high-frequency PWM pulses, resulting in an increased switching loss and hence the reduced efficiency.

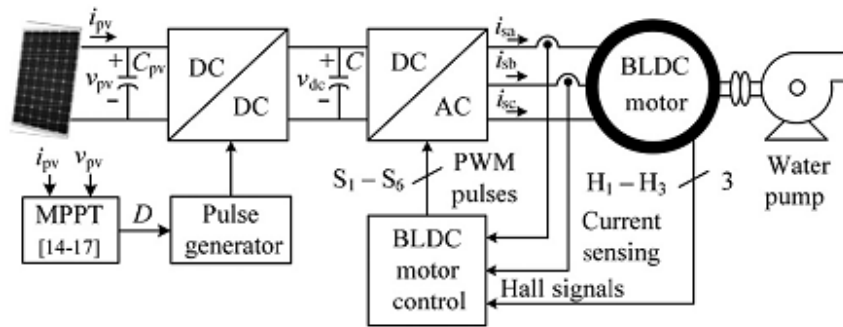


Fig.3.1. Conventional SPV-fed BLDC motor-driven water pumping system

Although a Z-source inverter (ZSI) replaces dc–dc converter in[22], other schematic of Fig.3.1 remains unchanged, promising high efficiency and low cost. Contrary to it, ZSI also necessitates phase current and dc link voltage sensing resulting in the complex control and increased cost.

To overcome these problems and drawbacks, a simple, cost-effective, and efficient water pumping system based on SPV array-fed BLDC motor is proposed, by modifying the existing topology (Fig. 1) as shown in Fig.3.2. A zeta converter is utilized to extract the maximum power available from an SPV array, soft starting, and speed control of BLDC motor coupled to a water pump. Due to a single switch, this converter has very good efficiency and offers boundless region for MPPT. This converter is operated in continuous conduction mode (CCM) resulting in a reduced stress on its power devices and components. Furthermore, the switching loss of VSI is reduced by adopting fundamental frequency switching resulting in an additional power saving and hence an enhanced efficiency. The phase currents as well as the dc link voltage sensors are completely eliminated, offering simple and economical system without sacrificing its performance. The speed of BLDC motor is controlled, without any additional control, through a variable dc link voltage of VSI. Moreover, a soft starting of BLDC motor is achieved by proper initialization of MPPT algorithm of SPV array. These features offer an increased simplicity of proposed system.

The advantages and desirable features of both zeta converter and BLDC motor drive contribute to develop a simple, efficient, cost-effective, and reliable water pumping system based on solar PV energy. Simulation results using MATLAB/Simulink and experimental performances are examined to demonstrate the starting, dynamics, and steady-state behavior of proposed water pumping system subjected to practical operating conditions. The SPV array and BLDC motor are designed such that proposed system always exhibits good performance regardless of solar irradiance level.

### **3.2 CONFIGURATION OF PROPOSED SYSTEM**

The structure of proposed SPV array-fed BLDC motor driven water pumping system employing a zeta converter is shown in Fig.3.2. The proposed system consists of (left to right) an SPV array, a zeta converter, a VSI, a BLDC motor, and a water pump. The BLDC motor has an inbuilt encoder. The pulse generator is used to operate the zeta

converter. A step-by-step operation of proposed system is elaborated in Section 3.3 in detail.

### 3.3 OPERATION OF PROPOSED SYSTEM

The SPV array generates the electrical power demanded by the motor-pump. This electrical power is fed to the motor pump via a zeta converter and a VSI. The SPV array appears as a power source for the zeta converter as shown in Fig.3.2. Ideally, the same amount of power is transferred at the output of zeta converter which appears as an input source for the VSI. In practice, due to the various losses associated with a dc-dc converter [23], slightly less amount of power is transferred to feed the VSI. The pulse generator generates, through INCMPPT algorithm, switching pulses for insulated gate bipolar transistor (IGBT) switch of the zeta converter. The INC-MPPT algorithm uses voltage and current as feedback from SPV array and generates an optimum value of duty cycle. Further, it generates actual switching pulse by comparing the duty cycle with a high-frequency carrier wave. In this way, the maximum power extraction and hence the efficiency optimization of the SPV array is accomplished.

The VSI, converting dc output from a zeta converter into ac, feeds the BLDC motor to drive a water pump coupled to its shaft. The VSI is operated in fundamental frequency switching through an electronic commutation of BLDC motor assisted by its built-in encoder. The high frequency switching losses are thereby eliminated, contributing in an increased efficiency of proposed water pumping system.

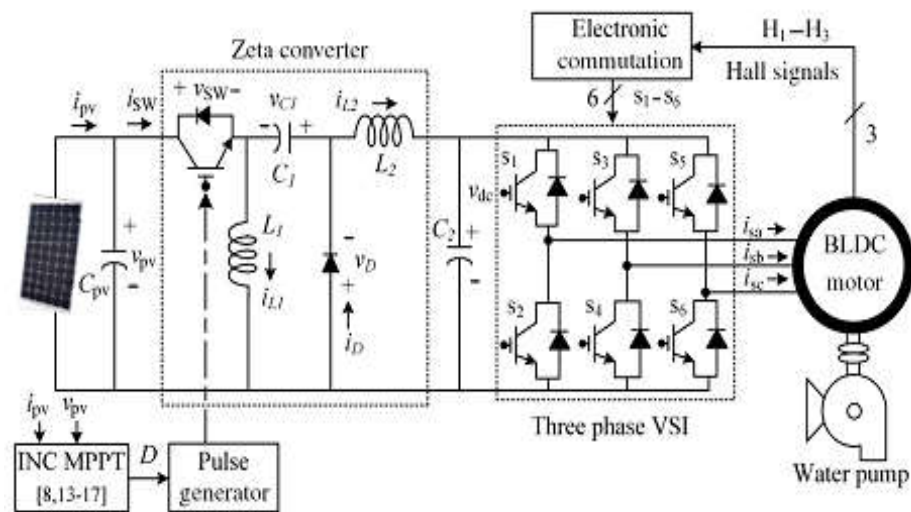


Fig.3.2. Proposed SPV-zeta converter-fed BLDC motor drive for water pump



### 3.4 DESIGN OF PROPOSED SYSTEM

Various operating stages shown in Fig.3.2 are properly designed to develop an effective water pumping system, capable of operating under uncertain conditions. A BLDC motor of 2.89-kW power rating and an SPV array of 3.4-kW peak power capacity under standard test conditions (STC) are selected to design the proposed system. The detailed designs of various stages such as SPV array, zeta converter, and water pump are described as follows.

#### 3.4.1 Design of SPV Array

As per above discussion, the practical converters are associated with various power losses. In addition, the performance of BLDC motor-pump is influenced by associated mechanical and electrical losses. To compensate these losses, the size of SPV array is selected with slightly more peak power capacity to ensure the satisfactory operation regardless of power losses. Therefore, the SPV array of peak power capacity of  $P_{mpp}=3.4$  kW under STC (STC: 1000 W/m<sup>2</sup>, 25°C, AM 1.5), slightly more than demanded by the motor-pump is selected and its parameters are designed accordingly. SolarWorld make Sunmodule Plus SW 280 mono [24] SPV module is selected to design the SPV array of an appropriate size. Electrical specifications of this module are listed in Table 3.1 and numbers of modules required to connect in series/parallel are estimated by selecting the voltage of SPV array at MPP under STC as  $V_{mpp}=187.2$  V.

TABLE 3.1  
Specifications of Sunmodule plus SW 280 mono SPV Module

Peak power, $P_m$ (W)	280
Open circuit voltage, $V_o$ (V)	39.5
Voltage at MPP, $V_m$ (V)	31.2
Short circuit current, $I_s$ (A)	9.71
Current at MPP, $I_m$ (A)	9.07
Number of cells connected in series, $N_{ss}$	60

The current of SPV array at MPP  $I_{mpp}$  is estimated as

$$I_{mpp} = P_{mpp}/V_{mpp} = 3400/187.2 = 18.16 \text{ A} \quad (3.1)$$

The numbers of modules required to connect in series are as follows:

$$N_s = V_{mpp}/V_m = 187.2/31.2 = 6. \quad (3.2)$$

The numbers of modules required to connect in parallel areas follows:

$$N_p = I_{mpp}/I_m = 18.16/9.07 = 2. \quad (3.3)$$

Connecting six modules in series, having two strings in parallel, an SPV array of required size is designed for the proposed system.

### 3.4.2 Design of Zeta Converter

The zeta converter is the next stage to the SPV array. Its design consists of an estimation of various components such as input inductor  $L_1$ , output inductor  $L_2$ , and intermediate capacitor  $C_1$ . These components are designed such that the zeta converter always operates in CCM resulting in reduced stress on its components and devices. An estimation of the duty cycle  $D$  initiates the design of zeta converter which is estimated as [6]

$$D = \frac{V_{dc}}{V_{dc} + V_{mpp}} = \frac{200}{200 + 187.2} = 0.52 \quad (3.4)$$

Where  $V_{dc}$  is an average value of output voltage of the zeta converter (dc link voltage of VSI) equal to the dc voltage rating of the BLDC motor.

An average current flowing through the dc link of the VSI  $I_{dc}$  is estimated as

$$I_{dc} = P_{mpp}/V_{dc} = 3400/200 = 17 \text{ A}. \quad (3.5)$$

Then,  $L_1$ ,  $L_2$ , and  $C_1$  are estimated as

$$L_1 = \frac{DV_{mpp}}{f_{sw}\Delta I_{L1}} = \frac{0.52 \times 187.2}{20000 \times 18.16 \times 0.06} = 4.5 \times 10^{-3} \approx 5 \text{ mH} \quad (3.6)$$

$$L_2 = \frac{(1-D)V_{dc}}{f_{sw}\Delta I_{L2}} = \frac{(1-0.52) \times 200}{20000 \times 17 \times 0.06} = 4.7 \times 10^{-3} \approx 5 \text{ mH} \quad (3.7)$$

$$C_1 = \frac{DI_{dc}}{f_{sw}\Delta V_{C1}} = \frac{0.52 \times 17}{20000 \times 200 \times 0.1} = 22 \text{ } \mu\text{F} \quad (3.8)$$

Where  $f_{sw}$  is the switching frequency of IGBT switch of the zeta converter;  $\Delta I_{L1}$  is the amount of permitted ripple in the current flowing through  $L_1$ , same as  $I_{L1} = I_{mpp}$ ;  $\Delta I_{L2}$  is

the amount of permitted ripple in the current flowing through  $L_2$ , same as  $I_{L2} = I_{dc}$ ;  $\Delta V_{C1}$  is permitted ripple in the voltage across  $C_1$ , same as  $V_{C1} = V_{dc}$ .

### 3.4.3 Estimation of DC-Link Capacitor of VSI

A new design approach for estimation of dc-link capacitor of the VSI is presented here. This approach is based on a fact that sixth harmonic component of the supply (ac) voltage is reflected on the dc side as a dominant harmonic in the three-phase supply system [25]. Here, the fundamental frequencies of output voltage of the VSI are estimated corresponding to the rated speed and the minimum speed of BLDC motor essentially required pumping the water. These two frequencies are further used to estimate the values of their corresponding capacitors. Out of these two estimated capacitors, larger one is selected to assure a satisfactory operation of proposed system even under the minimum solar irradiance level.

The fundamental output frequency of VSI corresponding to the rated speed of BLDC motor  $\omega_{rated}$  is estimated as

$$\omega_{rated} = 2\pi f_{rated} = 2\pi \frac{N_{rated} P}{120} = 2\pi \times \frac{3000 \times 6}{120} = 942 \text{ rad/s.} \quad (3.9)$$

The fundamental output frequency of the VSI corresponding to the minimum speed of the BLDC motor essentially required to pump the water ( $N = 1100 \text{ r/min}$ )  $\omega_{min}$  is estimated as

$$\omega_{min} = 2\pi f_{min} = 2\pi \frac{NP}{120} = 2\pi \times \frac{1100 \times 6}{120} = 345.57 \text{ rad/s} \quad (3.10)$$

Where  $f_{rated}$  and  $f_{min}$  are fundamental frequencies of output voltage of VSI corresponding to a rated speed and a minimum speed of BLDC motor essentially required to pump the water, respectively, in Hz;  $N_{rated}$  is rated speed of the BLDC motor;  $P$  is a number of poles in the BLDC motor.

The value of dc link capacitor of VSI at  $\omega_{rated}$  is as follows:

$$C_{2,rated} = \frac{I_{dc}}{6 \times \omega_{rated} \times \Delta V_{dc}} = \frac{17}{6 \times 942 \times 200 \times 0.1} = 150.4 \text{ } \mu\text{F.} \quad (3.11)$$

Similarly, a value of dc link capacitor of VSI at  $\omega_{min}$  is as follows:

$$C_{2,\min} = \frac{I_{dc}}{6 \times \omega_{\min} \times \Delta V_{dc}} = \frac{17}{6 \times 345.57 \times 200 \times 0.1} = 410 \mu F \quad (3.12)$$

Where  $\Delta V_{dc}$  is an amount of permitted ripple in voltage across dc-link capacitor  $C_2$ . Finally,  $C_2 = 410 \mu F$  is selected to design the dc-link capacitor.

### 3.4.4 Design of Water Pump

To estimate the proportionality constant  $K$  for the selected water pump, its power–speed characteristics [26], [27] is used as

$$K = \frac{P}{\omega_r^3} = \frac{2.89 \times 10^3}{(2\pi \times 3000/60)^3} = 9.32 \times 10^{-5} \quad (3.13)$$

Where  $P = 2.89$  kW is rated power developed by the BLDC motor and  $\omega_r$  is rated mechanical speed of the rotor (3000 r/min) in rad/s.

A water pump with these data is selected for proposed system.

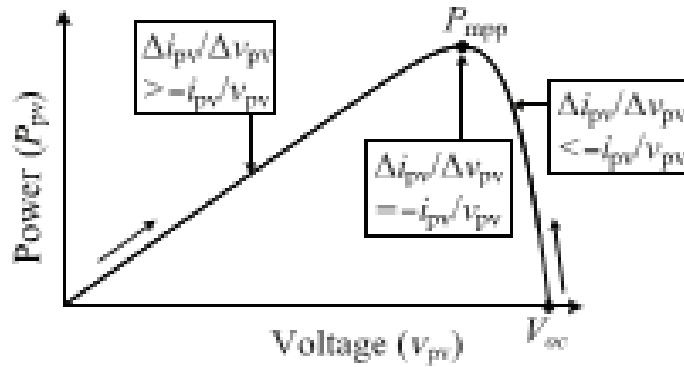


Fig.3.3. Illustration of INC-MPPT with SPV array  $P_{pv}$ – $v_{pv}$  characteristics.

TABLE 3.2

Switching States for Electronic Commutation of BLDC Motor

Rotor position $\theta$ (°)	Hall signals			Switching states					
	$H_3$	$H_2$	$H_1$	$S_1$	$S_2$	$S_3$	$S_4$	$S_5$	$S_6$
NA	0	0	0	0	0	0	0	0	0
0–60	1	0	1	1	0	0	1	0	0
60–120	0	0	1	1	0	0	0	0	1
120–180	0	1	1	0	0	1	0	0	1
180–240	0	1	0	0	1	1	0	0	0
240–300	1	1	0	0	1	0	0	1	0
300–360	1	0	0	0	0	0	1	1	0
NA	1	1	1	0	0	0	0	0	0

### 3.5 CONTROL OF PROPOSED SYSTEM

The proposed system is controlled in two stages. These two control techniques, viz., MPPT and electronic commutation, are discussed as follows.

#### 3.5.1 INC-MPPT Algorithm

An efficient and commonly used INC-MPPT technique [8],[13] in various SPV array based applications is utilized in order to optimize the power available from a SPV array and to facilitate a soft starting of BLDC motor. This technique allows perturbation in either the SPV array voltage or the duty cycle. The former calls for a proportional-integral (PI) controller to generate a duty cycle [8] for the zeta converter, which increases the complexity. Hence, the direct duty cycle control is adapted in this work. The INC-MPPT algorithm determines the direction of perturbation based on the slope of  $P_{pv}$ - $v_{pv}$  curve, shown in Fig.3.3. As shown in Fig.3.3, the slope is zero at MPP, positive on the left, and negative on the right of MPP, i.e.,

$$\left. \begin{aligned} \frac{dP_{pv}}{dv_{pv}} &= 0; & \text{at mpp} \\ \frac{dP_{pv}}{dv_{pv}} &> 0; & \text{left of mpp} \\ \frac{dP_{pv}}{dv_{pv}} &< 0; & \text{right of mpp} \end{aligned} \right\} \quad (3.14)$$

Since

$$\frac{dP_{pv}}{dv_{pv}} = \frac{d(v_{pv} * i_{pv})}{dv_{pv}} = i_{pv} + v_{pv} * \frac{di_{pv}}{dv_{pv}} \cong i_{pv} + v_{pv} * \frac{\Delta i_{pv}}{\Delta v_{pv}} \quad (3.15)$$

Therefore, (3.14) is rewritten as

$$\left. \begin{aligned} \frac{\Delta i_{pv}}{\Delta v_{pv}} &= -\frac{i_{pv}}{v_{pv}}; & \text{at mpp} \\ \frac{\Delta i_{pv}}{\Delta v_{pv}} &> -\frac{i_{pv}}{v_{pv}}; & \text{left of mpp} \\ \frac{\Delta i_{pv}}{\Delta v_{pv}} &< -\frac{i_{pv}}{v_{pv}}; & \text{right of mpp} \end{aligned} \right\} \quad (3.16)$$

Thus, based on the relation between INC and instantaneous conductance, the controller decides the direction of perturbation as shown in Fig. 3, and increases/decreases the duty cycle accordingly. For instance, on the right of MPP, the duty cycle is increased with a fixed perturbation size until the direction reverses. Ideally, the perturbation stops once the operating point reaches the MPP. However, in practice, operating point oscillates around the MPP.

As the perturbation size reduces, the controller takes more time to track the MPP of SPV array. An intellectual agreement between the tracking time and the perturbation size is held to fulfill the objectives of MPPT and soft starting of BLDC motor. In order to achieve soft starting, the initial value of duty cycle is set as zero. In addition, an optimum value of perturbation size ( $\Delta D = 0.001$ ) is selected, which contributes to soft starting and also minimizes oscillations around the MPP.

### **3.5.2 Electronic Commutation of BLDC Motor**

The BLDC motor is controlled using a VSI operated through an electronic commutation of BLDC motor. An electronic commutation of BLDC motor stands for commutating the currents flowing through its windings in a predefined sequence using decoder logic. It symmetrically places the dc input current at the center of each phase voltage for  $120^\circ$ . Six switching pulses are generated as per the various possible combinations of three Hall-effect signals. These three Hall-effect signals are produced by an inbuilt encoder according to the rotor position.

A particular combination of Hall-effect signals is produced for each specific range of rotor position at an interval of  $60^\circ$  [5], [6]. The generation of six switching states with the estimation of rotor position is tabularized in Table II. It is perceptible that only two switches conduct at a time, resulting in  $120^\circ$  conduction mode of operation of VSI and hence the reduced conduction losses. Besides this, the electronic commutation provides fundamental frequency switching of the VSI; hence, losses associated with high-frequency PWM switching are eliminated. A motor power company makes BLDC motor [28] with inbuilt encoder is selected for proposed system and its detailed specifications are given in the Appendixes.

## CHAPTER 4

### MATLAB AND SIMULINK MODEL

#### 4.1 Introduction to MATLAB

##### ➤ ***MATLAB***

Initially developed by a lecturer in 1970's to help students learn linear algebra. It was later marketed and further developed under Math Works Inc. (founded in 1984) [www.mathworks.com](http://www.mathworks.com). MATLAB is a software package which can be used to perform analysis and solve mathematical and engineering problems. It has excellent programming features and graphics capability – easy to learn and flexible. Available in many operating systems – Windows, Macintosh, UNIX, DOS. It has several tool boxes to solve specific problems.

MATLAB (matrix laboratory) is a multi-paradigm numerical computing environment and fourth-generation programming language. A proprietary programming language developed by Math Works, MATLAB allows matrix manipulations, plotting of functions and data, implementation of algorithms, creation of user interfaces, and interfacing with programs written in other languages, including C, C++, Java, Fortran and Python.

Although MATLAB is intended primarily for numerical computing, an optional toolbox uses the MuPAD symbolic engine, allowing access to symbolic computing abilities. An additional package, Simulink, adds graphical multi-domain simulation and model-based design for dynamic and embedded systems.

##### ➤ ***SIMULINK***

Simulink, developed by Math Works, is a graphical programming environment for modeling, simulating and analyzing multi-domain dynamic systems. Its primary interface is a graphical block diagramming tool and a customizable set of block libraries. It offers tight integration with the rest of the MATLAB environment and can either drive MATLAB or be scripted from it. Simulink is widely used in automatic control and digital signal processing for multi-domain simulation and Model-Based Design.

Used to model, analyze and simulate dynamic systems using block diagrams. Fully integrated with MATLAB, easy and fast to learn and flexible. It has comprehensive

block library which can be used to simulate linear, non-linear or discrete systems – excellent research tools. C codes can be generated from Simulink models for embedded applications and rapid prototyping of control systems.

➤ ***Simulink and its Relation to MATLAB***

The MATLAB and Simulink environments are integrated into one entity, and thus we can analyze, simulate, and revise our models in either environment at any point. We invoke Simulink from within MATLAB.

MATLAB is an interactive programming language that can be used in many ways, including data analysis and visualization, simulation and engineering problem solving. It may be used as an interactive tool or as a high level programming language. It provides an effective environment for both the beginner and for the professional engineer and scientist. SIMULINK™ is an extension to MATLAB that provides an iconographic programming environment for the solution of differential equations and other dynamic systems.

The package is widely used in academia and industry. It is particularly well known in the following industries: aerospace and defence; automotive; biotech, pharmaceutical; medical; and communications. Specialist toolboxes are available for a diverse range of other applications, including statistical analysis, financial modelling, and image processing and so on. Furthermore, real time toolboxes allow for on-line interaction with engineering systems, ideal for data logging and control.

Building on MATLAB (the language of technical computing), Simulink provides a platform for engineers to plan, model, design, simulate, test and implement complex electromechanical, dynamic control, signal processing and communication systems. Simulink-Matlab combination is very useful for developing algorithms, GUI assisted creation of block diagrams and realization of interactive simulation based designs. The eleven chapters of the book demonstrate the power and capabilities of Simulink to solve engineering problems with varied degree of complexity in the virtual environment.



## **4.2 Proposed work:**

### **4.2.1 Importance of Fuzzy Logic**

Fuzzy logic is all about the relative importance of precision: use as Fuzzy Logic Toolbox software with MATLAB technical computing software as a tool for solving problems with fuzzy logic. Fuzzy logic is a fascinating area of research because it does a good job of trading off between significance and precision something that humans have been managing for a very long time.

In this sense, fuzzy logic is both old and new because, although the modern and methodical science of fuzzy logic is still young, the concept of fuzzy logic relies on age-old skills of human reasoning.

### **4.2.2 Usage of Fuzzy Logic**

Fuzzy logic is a convenient way to map an input space to an output space. Mapping input to output is the starting point for everything. Consider the following examples:

- With information about how good your service was at a restaurant, a fuzzy logic system can tell you what the tip should be.
- With your specification of how hot you want the water, a fuzzy logic system can adjust the faucet valve to the right setting.
- With information about how far away the subject of your photograph is, a fuzzy logic system can focus the lens for you.
- With information about how fast the car is going and how hard the motor is working, a fuzzy logic system can shift gears for you.

To determine the appropriate amount of tip requires mapping inputs to the appropriate outputs. Between the input and the output, the preceding figure shows a black box that can contain any number of things: fuzzy systems, linear systems, expert systems, neural networks, differential equations, interpolated multidimensional lookup tables, or even a spiritual advisor, just to name a few of the possible options. Clearly the list could go on and on.

Of the dozens of ways to make the black box work, it turns out that fuzzy is often the very best way. As LotfiZadeh, who is considered to be the father of fuzzy logic, once remarked: "In almost every case you can build the same product without fuzzy logic, but fuzzy is faster and cheaper".

#### **4.2.3 Convenience of Fuzzy Logic**

Fuzzy logic is not a cure-all. When should you not use fuzzy logic? The safest statement is the first one made in this introduction: fuzzy logic is a convenient way to map an input space to an output space. Fuzzy logic is the codification of common sense — use common sense when you implement it and which will probably make the right decision. Many controllers, for example, do a fine job without using fuzzy logic. However, it take the time to become familiar with fuzzy logic, it can be a very powerful tool for dealing quickly and efficiently with imprecision and nonlinearity.

#### **4.2.4 The Fuzzy Logic Concept**

Fuzzy logic arose from a desire to incorporate logical reasoning and the intuitive decision making of an expert operator into an automated system. The aim is to make decisions based on a number of learned or predefined rules, rather than numerical calculations. Fuzzy logic incorporates a rule-base structure in attempting to make decisions. However, before the rule-base can be used, the input data should be represented in such a way as to retain meaning, while still allowing for manipulation. Fuzzy logic is an aggregation of rules, based on the input state variables condition with a corresponding desired output. A mechanism must exist to decide on which output, or combination of different outputs, will be used since each rule could conceivably result in a different output action.

Fuzzy logic can be viewed as an alternative form of input=output mapping. Consider the input premise,  $x$ , and a particular qualification of the input  $x$  represented by  $A_i$ . Additionally, the corresponding output,  $y$ , can be qualified by expression  $C_i$ . Thus, a fuzzy logic representation of the relationship between the input  $x$  and the output  $y$  could be described by the following:

R1: IF  $x$  is  $A_1$  THEN  $y$  is  $C_1$

R2: IF x is A2 THEN y is C2

.....

.....

.....

Rn: IF x is An THEN y is Cn

where x is the input (state variable), y is the output of the system,  $A_i$  are the different fuzzy variables used to classify the input x and  $C_i$  are the different fuzzy variables used to classify the output y. The fuzzy rule representation is linguistically based.

Thus, the input x is a linguistic variable that corresponds to the state variable under consideration. Furthermore, the elements  $A_i$  are fuzzy variables that describe the input x. Correspondingly, the elements  $C_i$  are the fuzzy variables used to describe the output y. In fuzzy logic control, the term “linguistic variable” refers to whatever state variables the system designer is interested in. Linguistic variables that are often used in control applications include Speed, Speed Error, Position, and Derivative of Position Error. The fuzzy variable is perhaps better described as a fuzzy linguistic qualifier. Thus the fuzzy qualifier performs classification (qualification) of the linguistic variables. The fuzzy variables frequently employed include Negative Large, Positive Small and Zero. Several papers in the literature use the term “fuzzy set” instead of “fuzzy variable”, however; the concept remains the same. Table 4.1 illustrates the difference between fuzzy variables and linguistic variables. Once the linguistic and fuzzy variables have been specified, the complete inference system can be defined. The fuzzy linguistic universe, U, is defined as the collection of all the fuzzy variables used to describe the linguistic variables.

i.e. the set U for a particular system could be comprised of Negative Small (NS), Zero (ZE) and Positive Small (PS). Thus, in this case the set U is equal to the set of [NS, ZE, PS]. For the system described by , the linguistic universe for the input x would be the set  $U_x = A_1 A_2 \dots A_n$ . Similarly,

TABLE 4.1 Fuzzy and linguistic variables

Linguistic Variables		Fuzzy Variables (Linguistic Qualifiers)	
Speed error	(SE)	Negative large	(NL)
Position error	(PE)	Zero	(ZE)
Acceleration	(AC)	Positive medium	(PM)
Derivative of position error	(DPE)	Positive very small	(PVS)
Speed	(SP)	Negative medium small	(NMS)

The linguistic universe for the output  $y$  would be the set  $U_y = \{C_1, C_2, \dots, C_n\}$ .

The Fuzzy Inference System (FIS) The basic fuzzy inference system (FIS) can be classified as: Type 1 Fuzzy Input Fuzzy Output (FIFO)

Type 2 Fuzzy Input Crisp Output (FICO)

Type 2 differs from the first in that the crisp output values are predefined and, thus, built into the inference engine of the FIS. In contrast, type 1 produces linguistic outputs. Type 1 is more general than type 2 as it allows redefinition of the response without having to redesign the entire inference engine. One drawback is the additional step required, converting the fuzzy output of the FIS to a crisp output. Developing a FIS and applying it to a control problem involves several steps:

1. Fuzzification
2. Fuzzy rule evaluation (fuzzy inference engine)
3. Defuzzification.

The total fuzzy inference system is a mechanism that relates the inputs to a specific output or set of outputs. First, the inputs are categorized linguistically (fuzzification), then the linguistic inputs are related to outputs (fuzzy inference) and, finally, all the different outputs are combined to produce a single output (defuzzification). Figure 4.1 shows a block diagram of the fuzzy inference system.

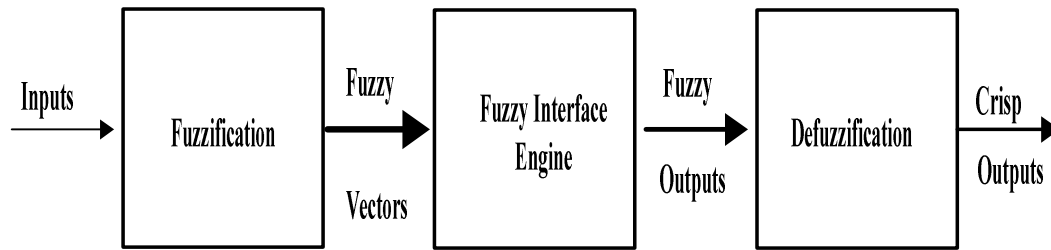


Fig .4.1 Fuzzy inference system

#### 4.2.5 Fuzzification:

Fuzzy logic uses linguistic variables instead of numerical variables. In a control system, error between reference signal and output signal can be assigned as Negative Big (NB), Negative Medium (NM), Negative Small (NS), Zero (ZE), Positive small (PS), Positive Medium (PM), Positive Big (PB). The triangular membership function is used for fuzzifications. The process of fuzzification convert numerical variable (real number) to a linguistic variable (fuzzy number).

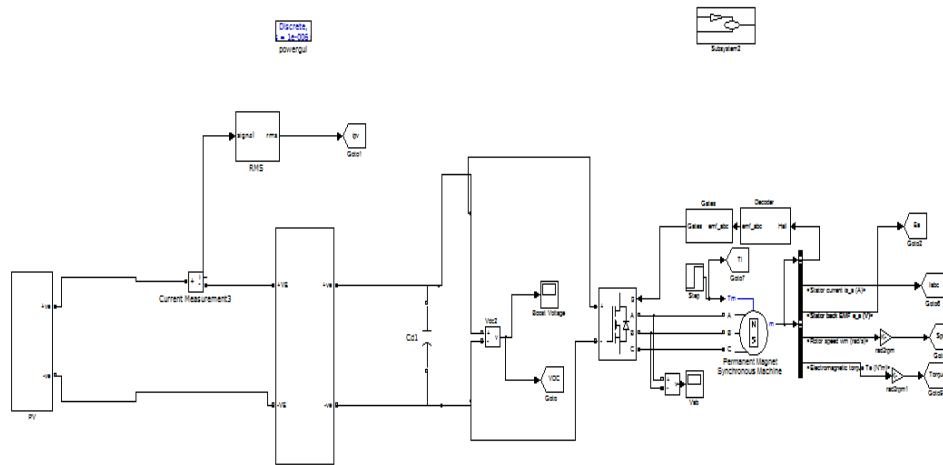
#### 4.2.6.Defuzzification:

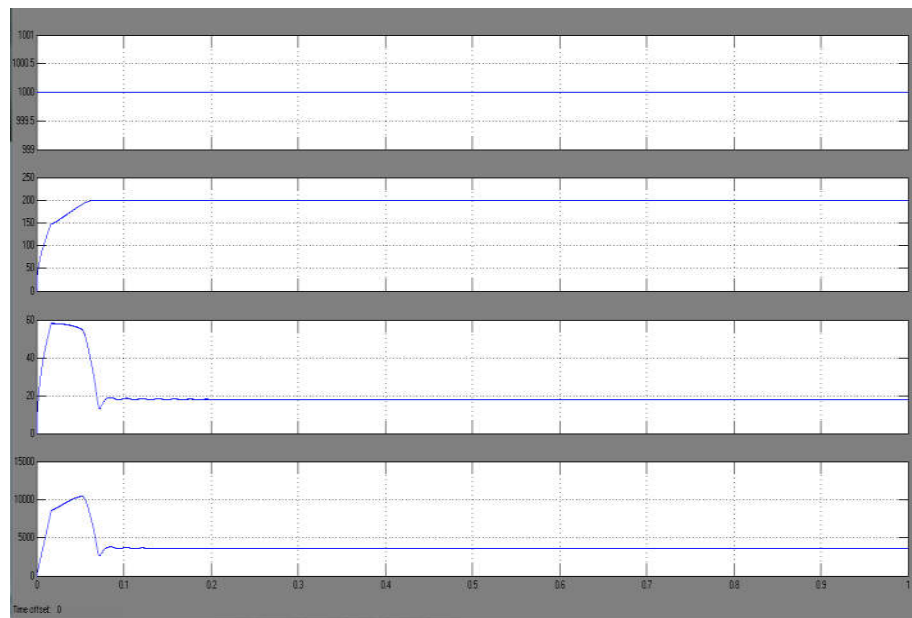
The rules of fuzzy logic controller generate required output in a linguistic variable (Fuzzy Number), according to real world requirements; linguistic variables have to be transformed to crisp output (Real number). This selection of strategy is a compromise between accuracy and computational intensity.

#### 4.2.7 Fuzzy Logic Controller

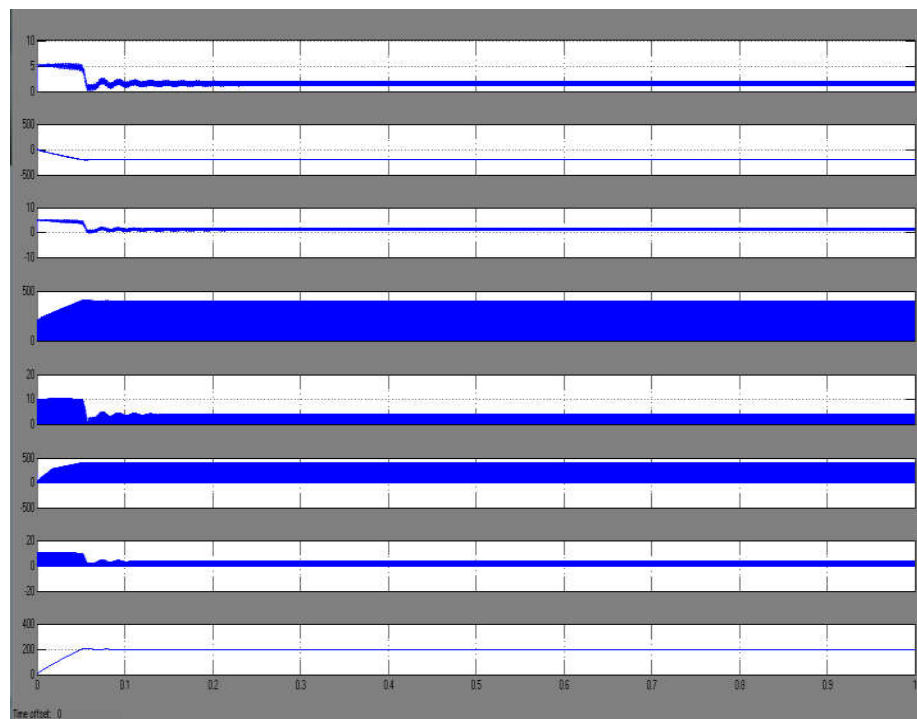
Fuzzy logic is a method of rule-based decision making used for expert systems and process control that emulates the rule-of-thumb thought process used by human beings. The basis of fuzzy logic is fuzzy set theory which was developed by LotfiZadeh in the 1960s. Fuzzy set theory differs from traditional Boolean (or two-valued) set theory in that partial membership in a set is allowed. Traditional Boolean set theory is two-valued in the sense that a member belongs to a set or does not and is represented by 1 or 0, respectively. Fuzzy set theory allows for partial membership, or a degree of membership, which might be any value along the continuum of 0 to 1. A linguistic term can be defined quantitatively by a type of fuzzy set known as a membership function. The

membership function specifically defines degrees of membership based on a property such as temperature or pressure. With membership functions defined for controller or expert system inputs and outputs, the formulation of a rule base of IF-THEN type conditional rules is done. Such a rule base and the corresponding membership functions are employed to analyze controller inputs and determine controller outputs by the process of fuzzy logic inference. By defining such a fuzzy controller, process control can be implemented quickly and easily. Many such systems are difficult or impossible to model mathematically, which is required for the design of most traditional control algorithms. In addition, many processes that might or might not be modeled mathematically are too complex or nonlinear to be controlled with traditional strategies. However, if a control strategy can be described qualitatively by an expert, fuzzy logic can be used to define a controller that emulates the heuristic rule-of-thumb strategies of the expert. Therefore, fuzzy logic can be used to control a process that a human can control manually with expertise gained from experience. The linguistic control rules that a human expert can describe in an intuitive and general manner can be directly translated to a rule base for a fuzzy logic controller.

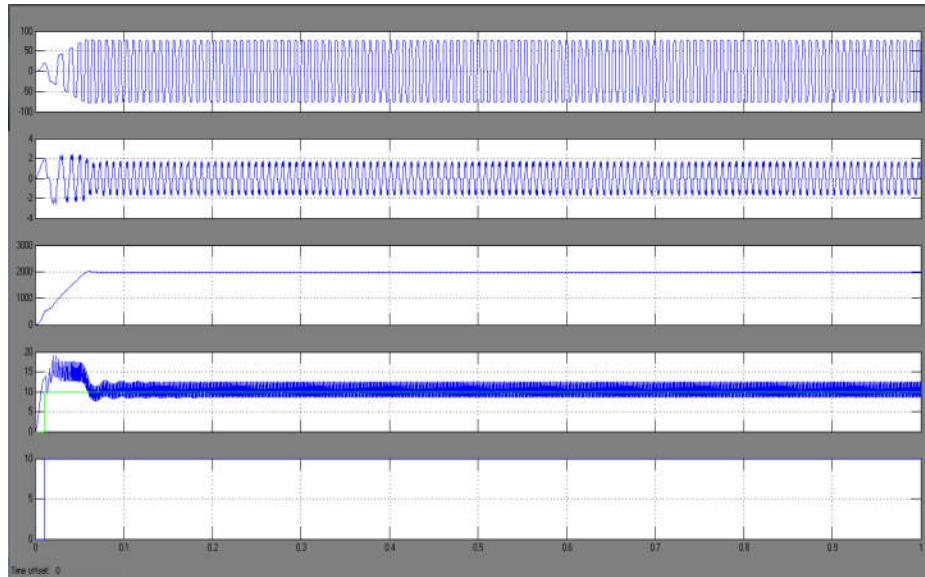




(a)



(b)



(c)

Fig.4.3 Starting and steady-state performances of the proposed SPV arraybased zeta converter-fed BLDC motor drive for water pump. (a) SPV arrayvariables. (b) Zeta converter variables. (c) BLDC motor-pump variables.

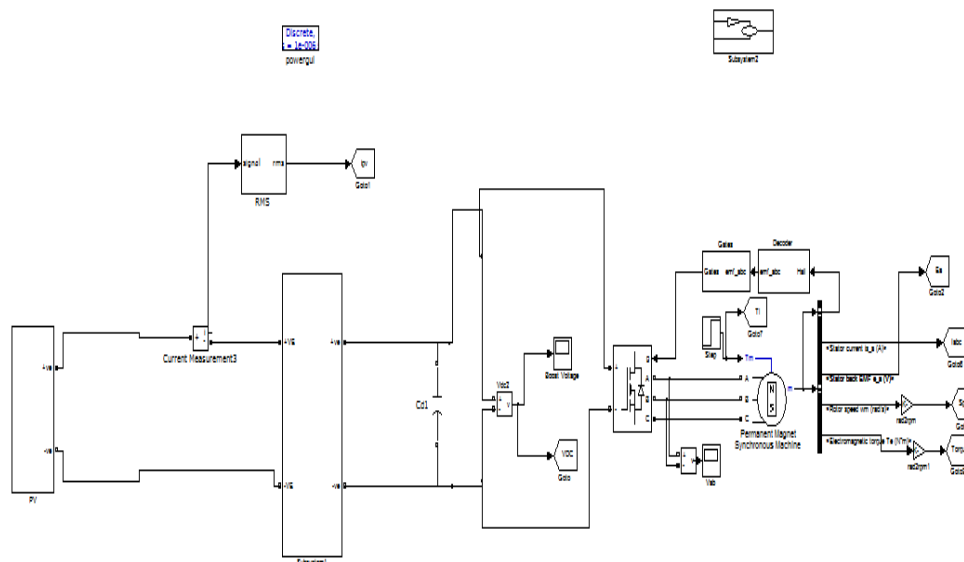
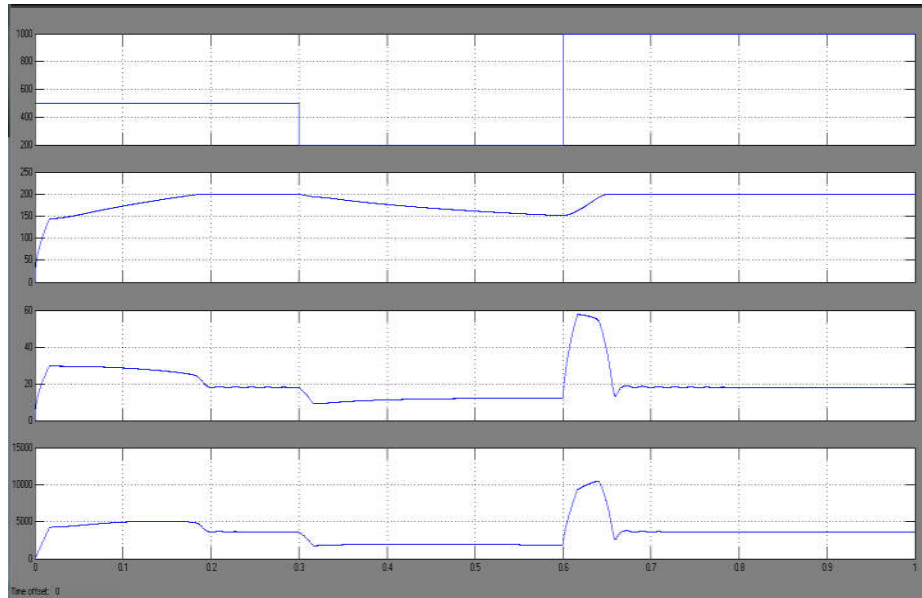
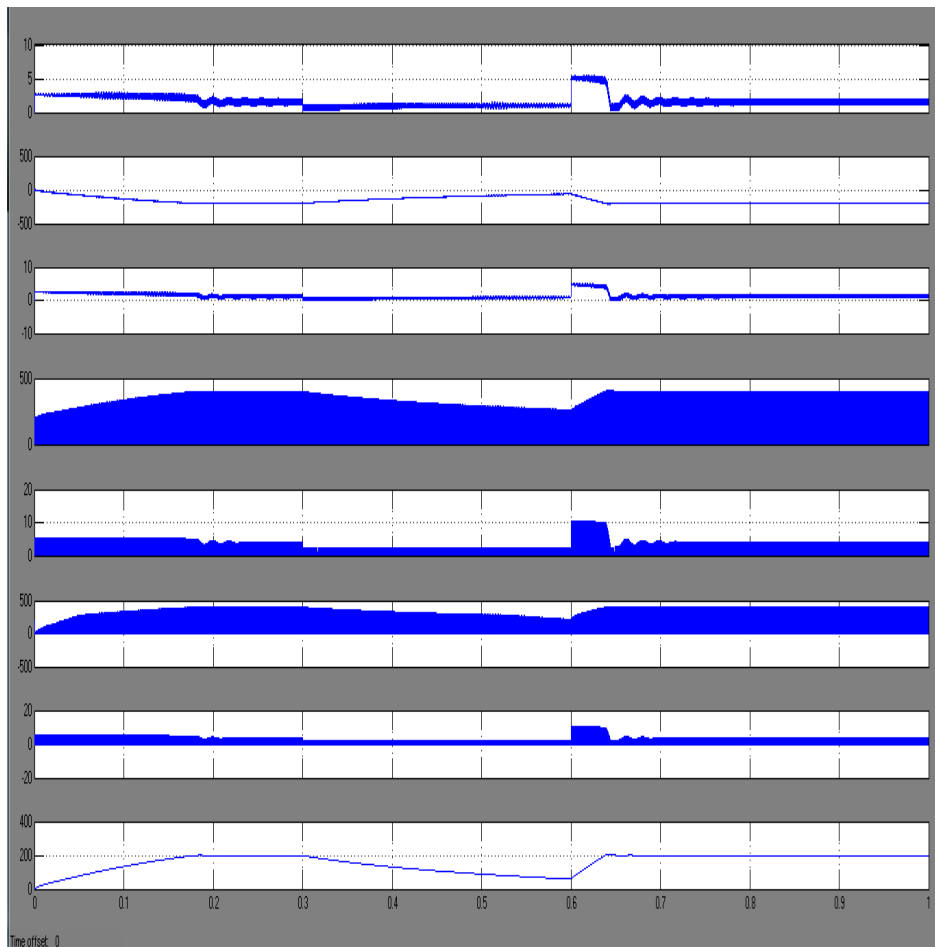


Fig 4.4Matlab/Simulink circuit for Dynamic performance of SPV array-based zetaconverter-fed BLDC motor drive for water pump

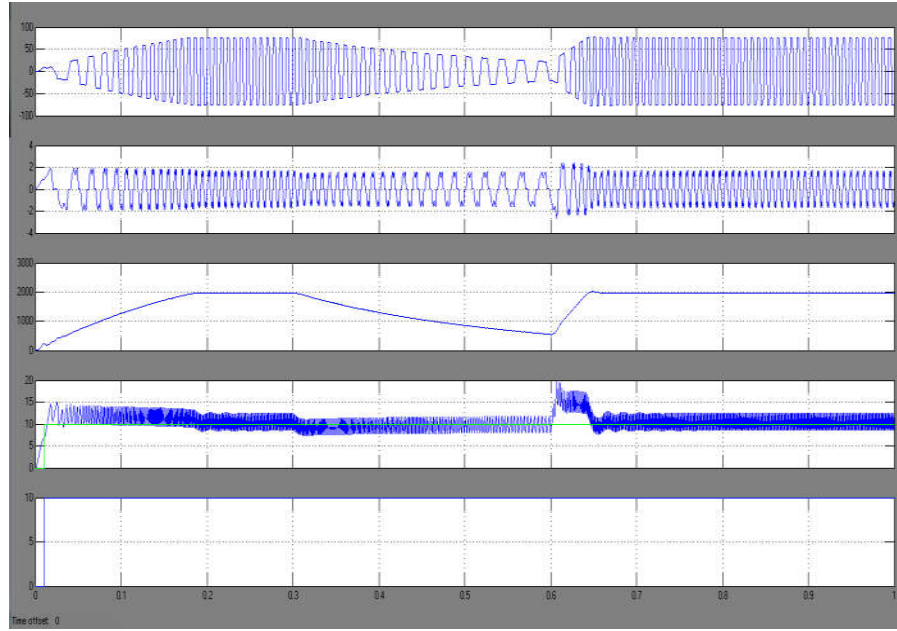




(a)



(b)



(c)

Fig.4.5. Dynamic performances of the proposed SPV array-based zeta converter-fed BLDC motor drive for water pump. (a) SPV array variables. (b) Zeta converter variables. (c) BLDC motor-pump variables.

## **CHAPTER 5**

### **CONCLUSION**

The SPV array-zeta converter-fed VSI–BLDC motor-pump has been proposed and its suitability has been demonstrated through simulated results and experimental validation. The proposed system has been designed and modeled appropriately to accomplish the desired objectives and validated to examine various performances under starting, dynamic, and steady-state conditions. The performance evaluation has justified the combination of zeta converter and BLDC motor for SPV array-based water pumping. The system under study has shown various desired functions such as maximum power extraction of the SPV array, soft starting of BLDC motor, fundamental frequency switching of VSI resulting in a reduced switching losses, speed control of BLDC motor without any additional control, and an elimination of phase current and dc-link voltage sensing, resulting in the reduced cost and complexity. The proposed system has operated successfully even under minimum solar irradiance.

## REFERENCES

- [1] M. Uno and A. Kukita, "Single-switch voltage equalizer using multistacked buck–boost converters for partially-shaded photovoltaic modules," *IEEE Trans. Power Electron.*, vol. 30, no. 6, pp. 3091–3105, Jun. 2015.
- [2] R. Arulmurugan and N. Suthanthiravanitha, "Model and design of a fuzzy-based Hopfield NN tracking controller for standalone PV applications," *Elect. Power Syst. Res.*, vol. 120, pp. 184–193, Mar. 2015.
- [3] S. Satapathy, K. M. Dash, and B. C. Babu, "Variable step size MPPT algorithm for photo voltaic array using zeta converter—A comparative analysis," in *Proc. Students Conf. Eng. Syst. (SCES)*, Apr. 12–14, 2013, pp. 1–6.
- [4] R. Kumar and B. Singh, "BLDC motor driven solar PV array fed waterpumping system employing zeta converter," in *Proc. 6th IEEE India Int. Conf. Power Electron. (IICPE)*, Dec. 8–10, 2014, pp. 1–6.
- [5] B. Singh, V. Bist, A. Chandra, and K. Al-Haddad, "Power factor correction in bridgeless-Luo converter-fed BLDC motor drive," *IEEE Trans. Ind. Appl.*, vol. 51, no. 2, pp. 1179–1188, Mar./Apr. 2015.
- [6] B. Singh and V. Bist, "Power quality improvements in a zeta converter for brushless dc motor drives," *IET Sci. Meas. Technol.*, vol. 9, no. 3, pp. 351–361, May 2015.
- [7] R. F. Coelho, W. M. dos Santos, and D. C. Martins, "Influence of power converters on PV maximum power point tracking efficiency," in *Proc. 10th IEEE/IAS Int. Conf. Ind. Appl. (INDUSCON)*, Nov. 5–7, 2012, pp. 1–8.
- [8] M. A. Elgendy, B. Zahawi, and D. J. Atkinson, "Assessment of the incremental conductance maximum power point tracking algorithm," *IEEE Trans. Sustain. Energy*, vol. 4, no. 1, pp. 108–117, Jan. 2013.
- [9] M. Sitbon, S. Schacham, and A. Kuperman, "Disturbance observer based voltage regulation of current-mode-boost-converter-interfaced photovoltaic generator," *IEEE Trans. Ind. Electron.*, vol. 62, no. 9, pp. 5776–5785, Sep. 2015.
- [10] R. Kumar and B. Singh, "Buck–boost converter fed BLDC motor drive for solar PV array based water pumping," in *Proc. IEEE Int. Conf. Power Electron. Drives Energy Syst. (PEDES)*, Dec. 16–19, 2014, pp. 1–6.

- [11] A. H. El Khateb, N. Abd. Rahim, J. Selvaraj, and B. W. Williams, "DCto-dc converter with low input current ripple for maximum photovoltaic power extraction," *IEEE Trans. Ind. Electron.*, vol. 62, no. 4, pp. 2246–2256, Apr. 2015.
- [12] D. D. C. Lu and Q. N. Nguyen, "A photovoltaic panel emulator using a buck–boost dc/dc converter and a low cost micro-controller," *Solar Energy*, vol. 86, no. 5, pp. 1477–1484, May 2012.
- [13] Z. Xuesong, S. Daichun, M. Youjie, and C. Deshu, "The simulation and design for MPPT of PV system based on incremental conductance method," in *Proc. WASE Int. Conf. Inf. Eng. (ICIE)*, Aug. 14–15, 2010, vol. 2, pp. 314–317.
- [14] A. R. Reisi, M. H. Moradi, and S. Jamasb, "Classification and comparison of maximum power point tracking techniques for photovoltaic system: A review," *Renew. Sustain. Energy Rev.*, vol. 19, pp. 433–443, Mar. 2013.
- [15] B. Bendib, H. Belmili, and F. Krim, "A survey of the most used MPPT methods: Conventional and advanced algorithms applied for photovoltaic systems," *Renew. Sustain. Energy Rev.*, vol. 45, pp. 637–648, May 2015.
- [16] B. Subudhi and R. Pradhan, "A comparative study on maximum power point tracking techniques for photovoltaic power systems," *IEEE Trans. Sustain. Energy*, vol. 4, no. 1, pp. 89–98, Jan. 2013.
- [17] M. A. G. de Brito, L. Galotto, L. P. Sampaio, G. de Azevedo e Melo, and C. A. Canesin, "Evaluation of the main MPPT techniques for photovoltaic applications," *IEEE Trans. Ind. Electron.*, vol. 60, no. 3, pp. 1156–1167, Mar. 2013.
- [18] K. S. Tey and S. Mekhilef, "Modified incremental conductance algorithm for photovoltaic system under partial shading conditions and load variation," *IEEE Trans. Ind. Electron.*, vol. 61, no. 10, pp. 5384–5392, Oct. 2014.
- [19] M. Ouada, M. S. Meridjet, and N. Talbi, "Optimization of photovoltaic pumping system based BLDC using fuzzy logic MPPT control," in *Proc. Int. Renew. Sustain. Energy Conf. (IRSEC)*, Mar. 7–9, 2013, pp. 27–31.
- [20] M. Dursun and S. Ozden, "Application of solar powered automatic water pumping in Turkey," *Int. J. Comput. Elect. Eng.*, vol. 4, no. 2, pp. 161–164, 2012.